Alternative splicing regulation of membrane trafficking genes during myogenesis

EMMA R. HINKLE,[1,2,7] HANNAH J. WIEDNER,[1,2,7] EDUARDO V. TORRES,[1] MICAELA JACKSON,[1] ADAM J. BLACK,[1] R. ERIC BLUE,[1] SARAH E. HARRIS,[3] BRYAN B. GUZMAN,[4] GABRIELLE M. GENTILE,[1,2] EUNICE Y. LEE,[1] YI-HSUAN TSAI,[5] JOEL PARKER,[2,5] DANIEL DOMINGUEZ,[4,5] and JIMENA GIUDICE[1,2,6]

[1]Department of Cell Biology and Physiology, The University of North Carolina at Chapel Hill, Chapel Hill, North Carolina 27599, USA
[2]Curriculum in Genetics and Molecular Biology (GMB), The University of North Carolina at Chapel Hill, Chapel Hill, North Carolina 27599, USA
[3]Department of Biochemistry and Biophysics, The University of North Carolina at Chapel Hill, Chapel Hill, North Carolina 27599, USA
[4]Department of Pharmacology, The University of North Carolina at Chapel Hill, Chapel Hill, North Carolina 27599, USA
[5]Lineberger Comprehensive Cancer Center, The University of North Carolina at Chapel Hill, Chapel Hill, North Carolina 27599, USA
[6]McAllister Heart Institute, School of Medicine, The University of North Carolina at Chapel Hill, Chapel Hill, North Carolina 27599, USA

ABSTRACT

Alternative splicing transitions occur during organ development, and, in numerous diseases, splicing programs revert to fetal isoform expression. We previously found that extensive splicing changes occur during postnatal mouse heart development in genes encoding proteins involved in vesicle-mediated trafficking. However, the regulatory mechanisms of this splicing-trafficking network are unknown. Here, we found that membrane trafficking genes are alternatively spliced in a tissue-specific manner, with striated muscles exhibiting the highest levels of alternative exon inclusion. Treatment of differentiated muscle cells with chromatin-modifying drugs altered exon inclusion in muscle cells. Examination of several RNA-binding proteins revealed that the poly-pyrimidine tract binding protein 1 (PTBP1) and quaking regulate splicing of trafficking genes during myogenesis, and that removal of PTBP1 motifs prevented PTBP1 from binding its RNA target. These findings enhance our understanding of developmental splicing regulation of membrane trafficking proteins which might have implications for muscle disease pathogenesis.

Keywords: alternative splicing; myogenesis; RNA-binding proteins; membrane trafficking

INTRODUCTION

Diverse transcripts and proteins arise from a limited genome through alternative splicing. Alternative splicing is a ubiquitous mechanism for tuning gene expression. In fact, approximately 95% of human genes are estimated to have at least one alternative isoform (Pan et al. 2008; Wang et al. 2008). The expression of particular splice variants contributes to transcript and protein diversity among different tissues. Previous work comparing the transcriptomes of different tissues revealed that skeletal muscle, brain, heart, and testes have highly tissue-specific and evolutionarily conserved splicing patterns (Merkin et al. 2012). Extensive alternative splicing changes occur during postnatal development of striated muscles in mice, with the majority of them occurring during the first 4 wk after birth in mice (Giudice et al. 2014; Brinegar et al. 2017). This developmental window coincides with a profound intracellular architectural transformation as the heart and skeletal muscles adapt to accommodate increased physiological demands (Franzini-Armstrong 1991; Xu et al. 2005; Olson 2006; Gokhin et al. 2008; Kalsotra et al. 2008).

Numerous splicing changes that arise during postnatal development of striated muscles occur in genes that encode proteins involved in vesicle-mediated transport and membrane dynamics (Giudice et al. 2014; Brinegar et al. 2017). The functional importance of these splice isoforms has been illustrated by studies demonstrating that expression of adult isoforms of trafficking genes are necessary for proper organization of transverse tubules (T-tubules),

[7]These authors contributed equally to this work.
Corresponding author: jimena_giudice@med.unc.edu
Article is online at http://www.rnajournal.org/cgi/doi/10.1261/rna.078993.121.

skeletal muscle force generation, and the development of skeletal muscle mass in mice (Fugier et al. 2011; Böhm et al. 2013; Giudice et al. 2016; Blue et al. 2018; Moulay et al. 2020).

In several cardiac and skeletal muscle disorders, adult tissues reexpress fetal splice isoforms that contribute to disease features (Du et al. 2010; Park et al. 2011; Ames et al. 2013). For example, in myotonic dystrophy type 1, splicing of membrane-related genes such as the chloride channel 1 (*CIC-1*), and bridging integrator 1 (*BIN1*) revert to fetal patterns (Wheeler et al. 2007; Fugier et al. 2011). Rescuing this mis-splicing restores muscle function in mouse models and in cultured human cells (Wheeler et al. 2007; Fugier et al. 2011). Despite the importance of membrane trafficking to normal striated muscle development and pathophysiology, the regulatory mechanisms underlying this membrane-trafficking splicing network are largely unknown.

A strong body of evidence indicates that splicing can be functionally coupled to transcription and influenced by local chromatin states (Alexander et al. 2010; Luco et al. 2010; Schor et al. 2013; Khan et al. 2014; Nojima et al. 2015; Agirre et al. 2021). Currently, very little is known regarding the role of chromatin in alternative splicing and membrane trafficking regulation in the context of striated muscle development. One previous study demonstrated that in cardiomyocytes calcium-induced hyperacetylation increases transcription rate and the skipping of developmentally regulated alternative exons (Sharma et al. 2014). Whether this mechanism applies to the splicing of membrane trafficking genes in striated muscle is unknown.

Numerous RNA-binding proteins (RBPs) act as splicing factors that coordinate alternative splicing during muscle development and are involved in the pathogenesis of muscular diseases. A combination of computational, in vitro, and in vivo studies suggest that the poly-pyrimidine tract binding proteins 1 and 2 (PTBP1 and PTBP2), quaking (QKI), RNA binding fox-1 homolog 2 (RBFOX2), muscleblind like proteins 1 and 2 (MBNL1 and MBNL2), and the CUGBP elav-like family members 1 and 2 (CELF1 and CELF2) are key splicing regulators in striated muscle development and myogenesis (Kalsotra et al. 2008; Hall et al. 2013; Batra et al. 2014; Giudice et al. 2014; Singh et al. 2014; Wang et al. 2015). However, almost nothing is known about which RBPs regulate the splicing of genes encoding proteins that control cellular functions related to membrane dynamics, endocytosis, and other intracellular transport steps.

In this study, we describe a set of splicing events in membrane trafficking genes that are characterized by tissue- and developmental stage-specific isoform expression patterns. We sought to determine the contribution of chromatin states, *cis*-regulatory sequences, and *trans*-acting RBPs to alternative splicing of these membrane trafficking genes during muscle cell differentiation. Given that proper splicing and intracellular transport are critical for striated muscle development and that correcting splicing can improve disease-associated muscle weakness, understanding the splicing regulatory mechanisms controlling the expression of genes encoding membrane trafficking proteins may be useful for therapeutic development.

RESULTS

Alternative splicing events in membrane trafficking genes

Membrane organization and intracellular transport are vital for the establishment of T-tubules and neuromuscular junctions, which are critical for heart and skeletal muscle function (Dowling et al. 2008; Al-Qusairi and Laporte 2011). Previously, we found that genes regulated by alternative splicing during postnatal mouse heart development are enriched for those encoding proteins involved in intracellular trafficking, endocytosis, and membrane dynamics (Giudice et al. 2014). Within the group of alternatively spliced membrane-related genes, we discovered that their functions fall into four subcategories: (i) clathrin-mediated endocytosis, (ii) structural proteins, (iii) other vesicle-mediated intracellular transport, and (iv) membrane curvature. For the current study, we selected 11 splicing events in 10 membrane-related genes (Fig. 1A) based on the following criteria: (i) at least two alternative splicing events were chosen from each subgroup to cover potentially different cellular functions; (ii) splicing events were chosen that were among the most pronounced in the previous study (Giudice et al. 2014). The clathrin heavy chain (CLTC), clathrin light chain (CLTA, also known as LCA), and the adaptor related protein complex 2 subunit alpha 1 (AP2A1) are involved in clathrin-mediated endocytosis. The capping actin protein of the muscle z-line subunit beta (CAPZB) and fibulin 2 (FBLN2) are two structural proteins. The transmembrane P24 trafficking protein 2 (TMED2), scribble (SCRIB), and the GTPase activating protein and VPS9 domains 1 (GAPVD1) are proteins involved in intracellular transport mediated by vesicles. Finally, the Cdc42 interacting protein 4 (TRIP10, also known as CIP4) and the formin binding protein 1 (FNBP1, also known as FB17) are both involved in membrane curvature and dynamics (Fig. 1A).

To understand how alternative splicing might influence the structure and potentially the function of membrane trafficking proteins, we utilized bioinformatic databases (Ensembl, Uniprot, and Interpro) to evaluate the protein domains and location of the alternative exon (Supplemental Fig. S1). The alternative exon of CLTC is located close to its trimerization domain (Supplemental Fig. S1A), which serves as a site of interaction with other clathrin chains to form the triskelion and the endocytic vesicles. The location of the alternative exon suggests that its inclusion could alter clathrin-coated vesicle assembly. Recent work has demonstrated that inclusion of the alternative exon of CLTC

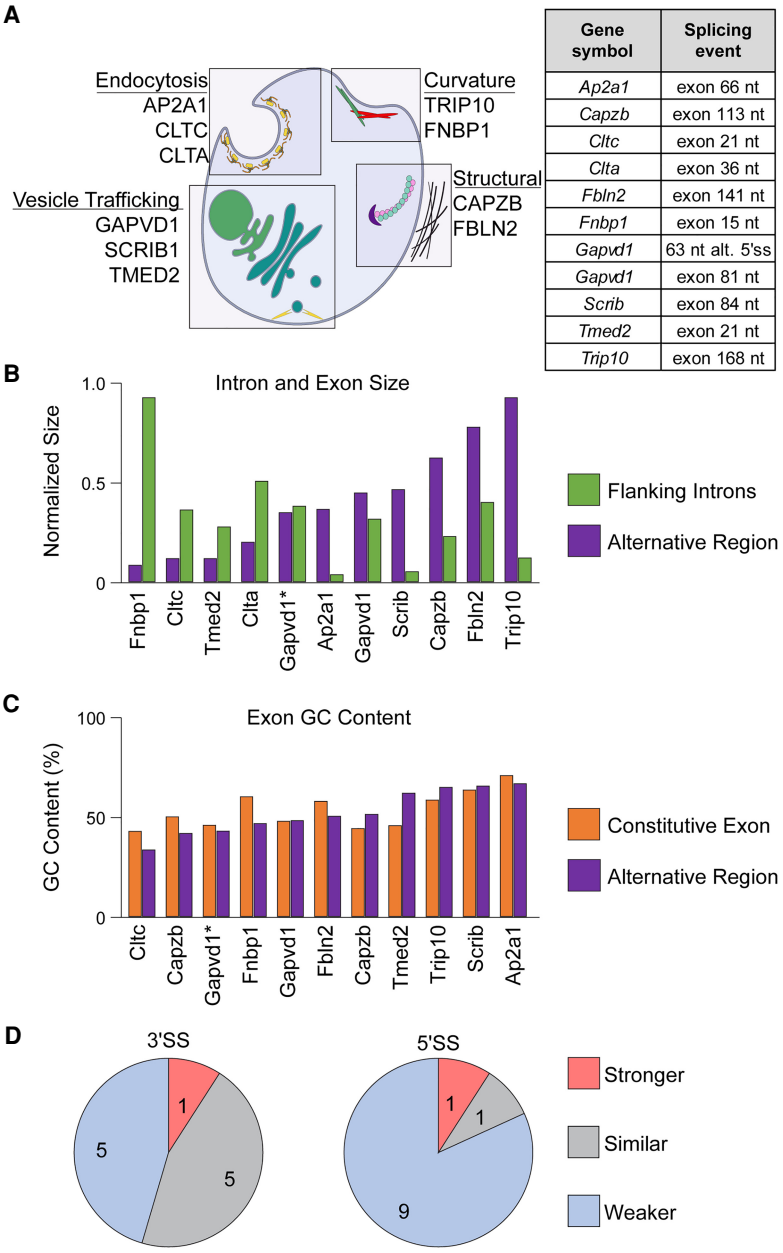

Gene symbol	Splicing event
Ap2a1	exon 66 nt
Capzb	exon 113 nt
Cltc	exon 21 nt
Clta	exon 36 nt
Fbln2	exon 141 nt
Fnbp1	exon 15 nt
Gapvd1	63 nt alt. 5'ss
Gapvd1	exon 81 nt
Scrib	exon 84 nt
Tmed2	exon 21 nt
Trip10	exon 168 nt

FIGURE 1. Characterization of a panel of splicing events in membrane trafficking genes. (*A*) Schematic representation of 10 proteins with functions related to membrane trafficking (*left*) and the size of the alternatively spliced region (*right*). (*B*) Relationship between the size of the alternative region and the sum of the sizes of the flanking introns. Sizes of the alternative region and the flanking intron were normalized to the largest exon or intron. *Gapvd1 denotes the alternative splice site (alt. 5′ss) in Gapvd1 pre-mRNA, which leads to an alternative region of 63 nt. (*C*) Quantification of GC content of alternative regions and their upstream constitutive exons. (*D*) Analysis of the strength of the alternative splice sites as scored by MaxEntScan. Stronger and weaker alternative splice sites were defined as those with a score 10% higher or lower than their corresponding constitutive splice sites, respectively.

dictates the organization of clathrin coats (Moulay et al. 2020). Interestingly, AP2A1, which binds clathrin to facilitate interactions with membrane components, and CLTA, which interacts with CLTC to form the clathrin triskelion, are also alternatively spliced (Supplemental Fig. S1B,C). This evidence further indicates that clathrin-mediated endocytosis might be functionally regulated by the expression of alternative isoforms.

We observed that the alternative regions are proximal to or within coiled-coil domains in CLTA, FNBP1, SCRIB, TRIP10, TMED2, and CAPZB (Supplemental Fig. S1C–H). For example, inclusion of the alternative exon of TMED2 adds a seven amino acid, in-frame, peptide within its coiled-coil domain (Supplemental Fig. S1G). Coiled coil domains are often involved in vesicle tethering to the Golgi (Truebestein and Leonard 2016). Given that TMED2 is believed to be involved in transporting cargo between the endoplasmic reticulum and Golgi apparatus, it is possible that inclusion of the alternative region influences intracellular trafficking by TMED2 (Barr et al. 2001).

Inclusion of the alternative exon of CAPZB shifts the reading frame of the carboxyl terminus, which influences localization of the protein in heart (Supplemental Fig. S1H). CAPZB is a structural protein and is important for capping the growing actin filaments to prevent addition and degradation. The long CAPZB isoform containing the alternative exon localizes to the Z-line, whereas the short isoform is found in the intercalated discs of cardiomyocytes (Schafer et al. 1993). FBLN2 is another structural protein that is alternatively spliced (Danan-Gotthold et al. 2015). The alternative exon of FBLN2 encodes an EGF-like calcium binding domain (Supplemental Fig. S1I), which may influence its ability to bind calcium or its role as an extracellular matrix protein. Two alternative splicing events occur in GAPVD1 (Supplemental Fig. S1J,K). Inclusion of the alternative exon of GAPVD1 inserts a 27 amino acid peptide between the Ras GTP-ase (RGT) domain and the coiled coil domain (Supplemental Fig. S1J) and use of an alternative 5′ splice site adds a 21 amino acid peptide near the RGT domain (Supplemental Fig. S1K). The molecular functions of most of the alternative isoforms of membrane trafficking genes have not been examined, but they likely

influence protein function, and ultimately, membrane dynamics.

Sequence analysis of the alternative exons indicated that within the selected set of trafficking genes, short alternative exons were flanked by large intronic regions, whereas the long alternative exons were surrounded by shorter intronic regions (Fig. 1B). Furthermore, the GC-content of the alternative exons was similar to constitutive exons from the same gene (Fig. 1C) and the majority of the alternative 3′ and 5′ splice sites were similar to or weaker than their constitutive sites, as scored by MaxEntScan (Fig. 1D).

Membrane trafficking genes are regulated by alternative splicing in a tissue- and developmental stage-specific manner

Given that the splicing of several membrane trafficking genes is important for proper striated muscle architecture and function, (Fugier et al. 2011; Giudice et al. 2016; Blue et al. 2018; Moulay et al. 2020) we sought to define the expression patterns of alternative isoforms in various tissues during postnatal development. We collected 14 different organs from FVB–NJ mice at postnatal day 4.5 (p4.5) and adulthood (4 mo of age) and quantified the percent spliced in (PSI) of the alternative region for our panel of 11 splicing events using reverse transcription PCR (RT-PCR) assays. In adult mouse tissues, we observed that the isoforms including the alternative regions were expressed in heart, skeletal muscle, and some in brain, but not in the other evaluated tissues (Fig. 2A). The level of inclusion of the alternative regions was lower in neonatal heart and skeletal muscles when compared to the adult tissues but was still higher than in other neonatal tissues such as the spleen, kidney, and liver, among others (Supplemental Fig. S2). For example, the 168 nt containing exon of Trip10 pre-mRNA was not included or very lowly included in neonatal spleen, intestine (Fig. 2B, left), kidney, liver, brain, and lung (Supplemental Fig. S3A), while adult heart and skeletal muscle tissues exhibited high levels of inclusion (58% and 82%, respectively) (Fig. 2B, right; Supplemental Fig. S3A). Similarly, the 81 nt containing alternative exon of Gapvd1 pre-mRNA was very lowly included in neonatal spleen, intestine (Fig. 2C, left), kidney, liver, and lung (Supplemental Fig. S3B), but striated muscle tissues exhibited higher levels of inclusion (27% in heart and 36% in *gastrocnemius* muscle) compared to the other tissues, excluding brain (58%) (Fig 2C, right; Supplemental Fig. S3B). The 21

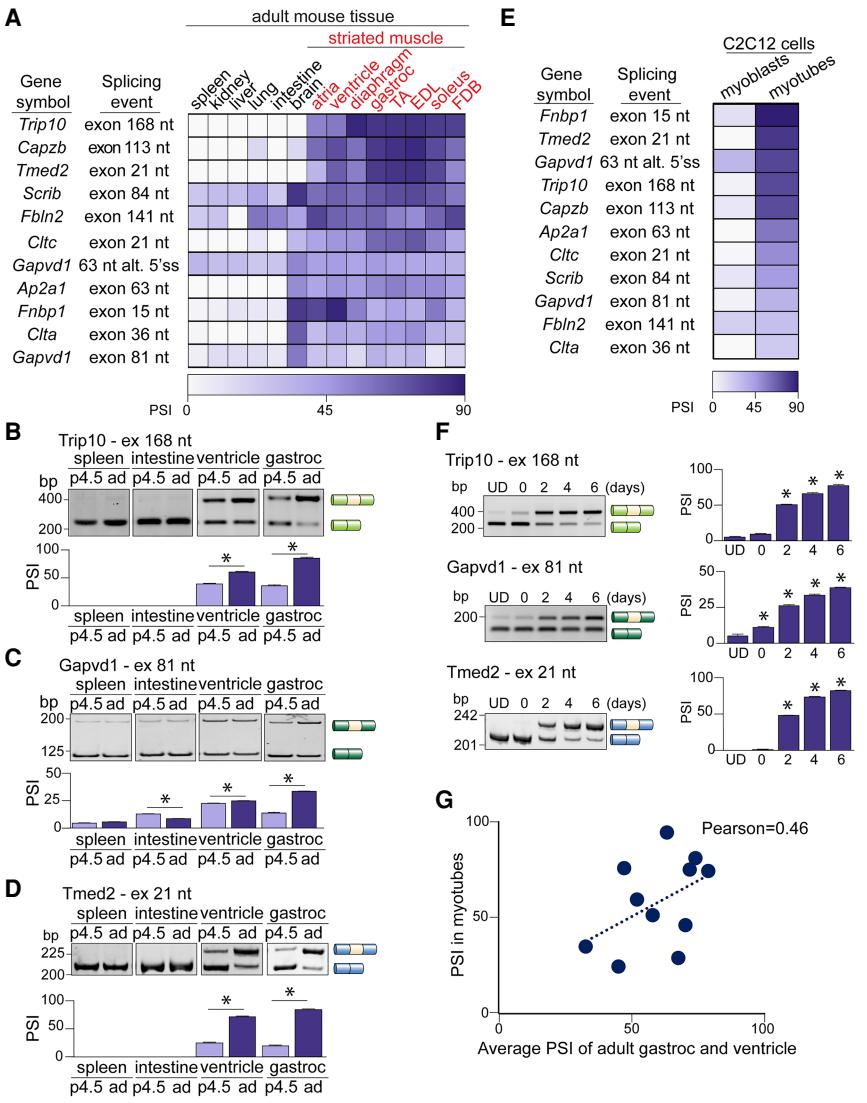

FIGURE 2. Membrane trafficking genes are regulated by alternative splicing in a tissue-specific manner and during C2C12 cell differentiation. (*A–D*) Alternative splicing of trafficking genes in mouse tissues was evaluated by RT-PCR and quantified by densitometry. Heatmap shows the summary of the results of 11 events in adult mice (*A*). Striated muscles are labeled in red. Three examples are shown: Trip10 (*B*), Gapvd1 (*C*), and Tmed2 (*D*) in neonatal (postnatal day 4.5, p4.5) and adult (ad) tissues. (*E*,*F*) Splicing of trafficking genes was evaluated during C2C12 cell differentiation. The heatmap summarizes the results of all the tested events (*E*). Splicing events in Trip10, Tmed2, and Gapvd1 pre-mRNAs are shown as examples (*F*). (*G*) Correlation plot between the PSI in myotubes and the average of adult skeletal *gastrocnemius* muscle and adult ventricle. Results are shown as mean ± SEM, $n = 3$, (*) $P < 0.05$, Welch's *t*-test, adult versus p4.5 or differentiated (D) versus undifferentiated (UD). (PSI) Percent spliced in, (EDL) extensor digitorum longus, (FDB) flexor digitorum brevis, (TA) tibialis anterior.

nt containing exon of Tmed2 pre-mRNA was completely excluded in spleen, intestine (Fig. 2D, left), kidney, liver, brain, and lung (Supplemental Fig. S3C), but included in adult heart and *gastrocnemius* muscle (68% and 80%, respectively) (Fig. 2D, right) and other skeletal muscle tissues (Supplemental Fig. S3C).

These studies led us to conclude that alternative splicing of membrane trafficking genes is regulated during postnatal development and their tissue-specific isoform expression suggests that the splice isoforms may contribute to the proper functionality of adult striated muscles.

Splicing transitions in membrane trafficking genes observed in vivo are robustly reproduced during C2C12 cell differentiation in vitro

C2C12 mouse myoblast cells are a well-established model used to study aspects of striated muscle biology in vitro (McMahon et al. 1994; Bland et al. 2010). Upon reduction of the serum concentration, mononucleated C2C12 myoblasts exit the cell cycle and fuse together to form multinucleated myotubes (myogenesis). We utilized existing RNA-sequencing data from C2C12 myoblasts and myotubes (Singh et al. 2014) to determine whether the splicing transitions in membrane trafficking genes observed during striated muscle development in vivo were recapitulated during C2C12 cell differentiation. Using the Mixture of Isoforms (MISO) software (Katz et al. 2010), we defined differentially alternatively spliced events as those exhibiting a $|\Delta PSI| \geq 0.1$ where ΔPSI was defined as the difference between the PSI in myotubes and the PSI in myoblasts. We detected 427 events with positive ΔPSI values ($\Delta PSI \geq 0.1$) and 231 events with negative ΔPSI values ($\Delta PSI \leq -0.1$), for a total of 658 events that were differentially spliced between myoblasts and myotubes. Gene ontology (GO) analysis (Yu et al. 2012) of these genes revealed an enrichment of endocytosis, trafficking and cell organization categories ($P < 8 \times 10^{-3}$) (Supplemental Fig. S3D). Thus, GO categories related to membrane dynamics and intracellular trafficking were prevalent in the global dataset of differentially spliced genes during myogenesis, consistent with observations made by us and others during in vivo development of the heart and skeletal muscle (Giudice et al. 2014; Brinegar et al. 2017). To validate these findings, we evaluated the splicing patterns of our 11 selected splicing events in C2C12 myoblasts and myotubes via RT-PCR (Fig. 2E,F). All of the alternative regions that transitioned from lower to higher inclusion levels during striated muscle development in mice also increased in inclusion during C2C12 cell differentiation in culture (Fig. 2E). Trip10 (exon of 168 nt), Gapvd1 (exon of 81 nt), and Tmed2 (exon of 21 nt) exhibited low inclusion (4%, 4%, 0%, respectively) in myoblasts and a gradual increase in inclusion levels up to 75%, 35%, 81%, respectively, after 6 d of differentiation (Fig. 2E,F).

The mean inclusion levels of alternative regions in adult skeletal *gastrocnemius* muscle and adult ventricle were positively correlated with their levels in differentiated C2C12 cells (myotubes) (Fig. 2G, Pearson = 0.46). These results indicate that differentiation of C2C12 cells recapitulate most in vivo splicing transitions, and they can serve as an appropriate model for investigating the molecular regulators controlling the striated muscle splicing transitions in membrane trafficking genes.

Chromatin-modifying drugs influence alternative splicing outputs in trafficking genes

Chromatin states can influence alternative splicing decisions both in cell culture and tissues (Luco et al. 2010; Khan et al. 2014; Xu et al. 2021). Thus, we sought to investigate if chromatin-modifying drugs influence alternative splicing decisions in membrane trafficking genes. After differentiating C2C12 cells for at least 72 h, we treated myotubes with trichostatin A (TSA) or camptothecin (CPT).

TSA is a histone deacetylase inhibitor that promotes a more permissive chromatin environment and has been demonstrated to facilitate transcriptional elongation in mammalian cell culture (Protacio et al. 2000; Bintu et al. 2012; Dujardin et al. 2014). After treating myotubes with TSA for 16–18 h, we observed an over threefold increase in histone acetylation (Fig. 3A). Splicing assays revealed a $|\Delta PSI| > 5$ in 8 of the 11 events in the developmentally regulated membrane trafficking genes (Fig. 3B–D). While alternative exons in Cltc and Tmed2 pre-mRNAs displayed drastic increases in skipping after TSA exposure (Fig. 3B, C), alternative exons in Fbln2 and Scrib pre-mRNAs showed an increase in inclusion levels (Fig. 3B,C). Overall, the primary response to histone acetylation was an increase in exon skipping (Fig. 3C,D) and exon size was correlated with TSA-responsive splicing changes (Pearson = 0.62) with the shortest exons having the highest degree of exon skipping (Fig. 3E).

We next treated myotubes for 16–18 h with CPT (1 or 10 μM), a potent topoisomerase inhibitor. One effect of CPT treatment is inhibition of transcriptional elongation, either by restricting unwinding of the supercoiled DNA template, or by inducing transcriptional pausing (Ljungman and Hanawalt 1996; Listerman et al. 2006). Exon skipping was increased in Cltc, Capzb, and Fnbp1 pre-mRNAs in response to CPT treatment (Fig. 3F,G). In fact, CPT treatment led to a dose-response increase in exon skipping for most membrane trafficking genes under investigation (Fig. 3G,H).

To determine whether overall mRNA expression was altered by TSA and CPT treatment, we performed quantitative real time PCR (qPCR) assays for our set of membrane trafficking genes. All mRNAs exhibited a significant upregulation at the mRNA level after TSA treatment except Trip10 (Supplemental Fig. S4). In contrast, Capzb, Fbln2,

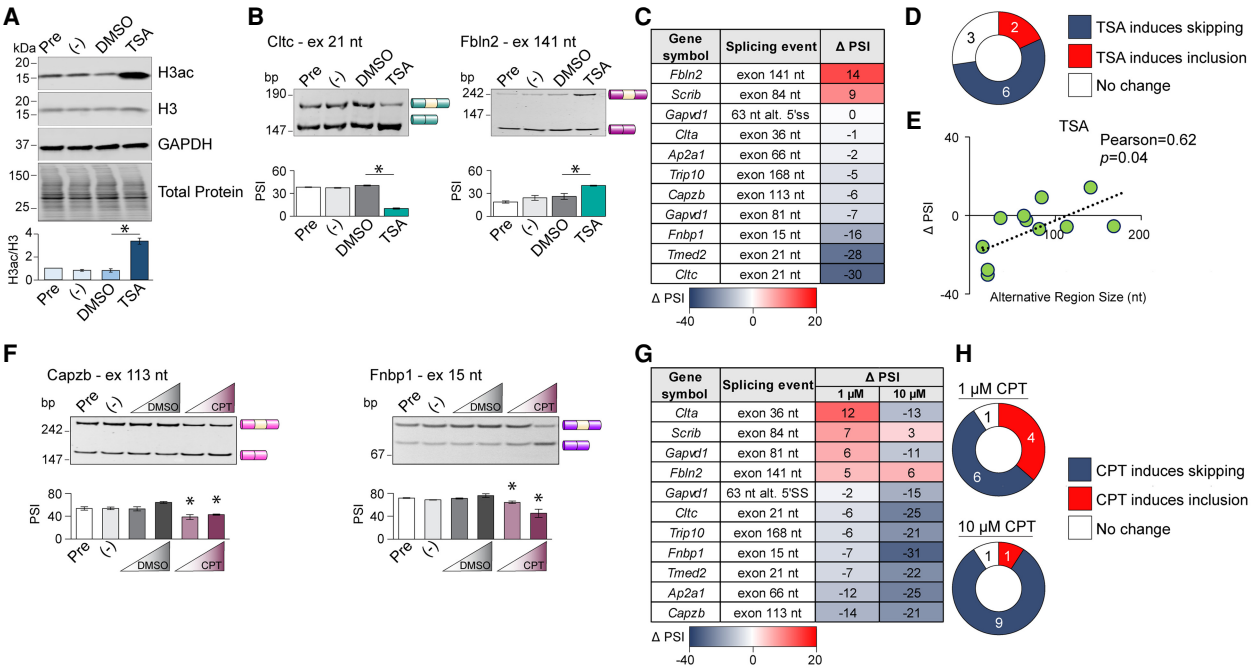

FIGURE 3. Trichostatin A (TSA) and camptothecin (CPT) treatment influence alternative splicing outputs. (*A*) Western blot assays were performed using lysates from myotubes treated with TSA. Untreated cells were collected before (Pre) and 16–18 h after (–) TSA treatment. The ratio of acetylated histone H3 (H3ac) to total histone H3 was quantified by densitometry. (*B*,*C*) After treatment with TSA, splicing of trafficking genes was determined in myotubes by RT-PCR and PSI was quantified via densitometry. (*D*) Pie chart of splicing events that respond to TSA treatment. Skipping and inclusion were defined as events with a $\Delta PSI \leq -5$ and $\Delta PSI \geq 5$, respectively. (*E*) Scatterplot of alternative region size and ΔPSI. (*F*,*G*) Myotubes were treated with CPT (1 or 10 μM), splicing of trafficking genes was evaluated by RT-PCR, and PSI was quantified via densitometry. (*H*) Pie chart of splicing events that respond to CPT treatment. ΔPSI was defined as the difference between the PSI under TSA or CPT treatment and the PSI when an equal volume of DMSO (vehicle) was added. Results are shown as mean ± SEM, $n = 3$–6, (*) $P < 0.05$, Welch's *t*-test, TSA or CPT treatment versus an equal volume of DMSO. (bp) Basepair, (DMSO) dimethyl sulfoxide, (KDa) kilodalton, (nt) nucleotide, (PSI) percent spliced in.

Fnbp1, Gapvd1, Scrib, and Tmed2 were down-regulated after CPT treatment. These results are not surprising given that TSA and CPT promote and inhibit overall transcription, respectively. We found no association between the up- or down-regulation of gene expression in response to TSA or CPT and the splicing outcomes. Because we observed similar splicing outcomes in response to TSA or CPT treatment (e.g., the alternative exon of Fnbp1 is skipped in response to both CPT and TSA treatment), overall gene expression does not appear to drive splicing changes.

Chromatin states are known to be coupled to splicing through the action of RBPs. Therefore, we next sought to determine the identities of RBPs that regulate the splicing of trafficking genes.

RBP expression changes during myogenesis

We selected a group of RBPs that were previously described as splicing regulators and that are known to be expressed in C2C12 cells, skeletal muscle, and heart tissue: PTBP1, PTBP2, RBFOX2, QKI, MBNL1, MBNL2, CELF1, and CELF2 (Bland et al. 2010; Wang et al. 2012; Hall et al. 2013; Giudice and Cooper 2014; Singh et al. 2014; Wang et al. 2015). First, we defined the expression patterns of these candidate RBPs in myoblasts and myotubes using western blot assays (Fig. 4A). Consistent with previous reports, we observed that PTBP1 was expressed in myoblasts but virtually absent in myotubes (Fig. 4B; Boutz et al. 2007; Bland et al. 2010). PTBP2, a homolog of PTBP1, was down-regulated by 49% during C2C12 cell differentiation (Fig. 4C). These findings are consistent with previous work that suggests PTBP2 repression occurs via miR-133 up-regulation during myogenesis (Boutz and Chawla 2007). RBFOX2 expression was 36% higher in myotubes compared with myoblasts (Fig. 4D), while QKI levels were unaltered during myogenesis (Fig. 4E). We observed similar expression levels of CELF1 and MBNL1 in myoblasts and myotubes, but a twofold increase in CELF2 expression and a 36% decrease in MBNL2 expression during differentiation (Fig. 4F–I).

These results led us to hypothesize that the expression dynamics of RBPs could influence the splicing of alternative exons in the membrane trafficking genes during myogenesis.

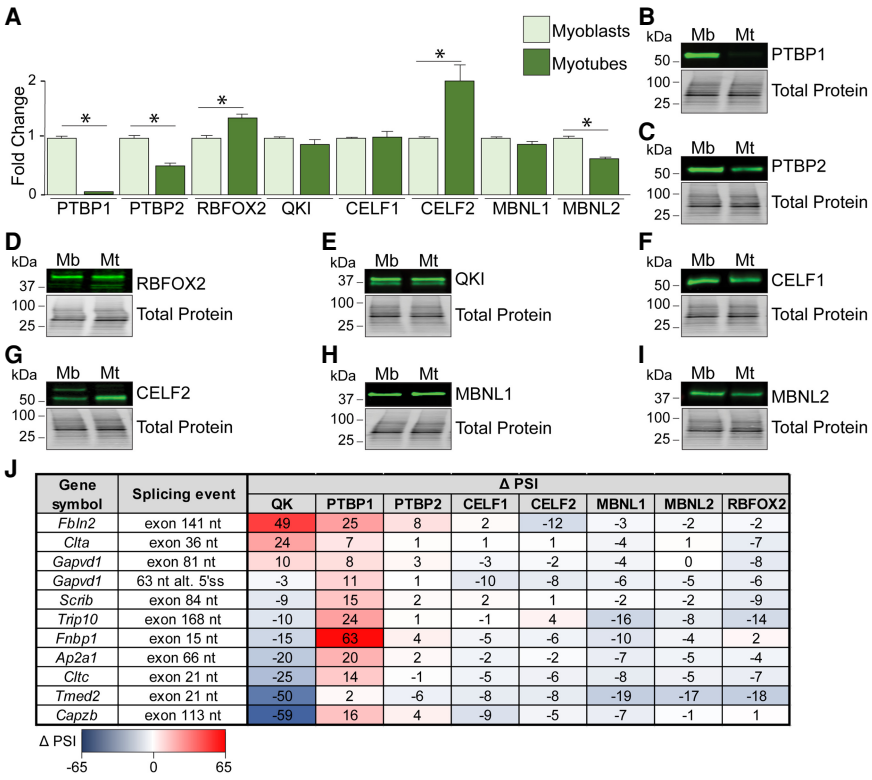

J

Gene symbol	Splicing event	Δ PSI							
		QK	PTBP1	PTBP2	CELF1	CELF2	MBNL1	MBNL2	RBFOX2
Fbln2	exon 141 nt	49	25	8	2	-12	-3	-2	-2
Clta	exon 36 nt	24	7	1	1	1	-4	1	-7
Gapvd1	exon 81 nt	10	8	3	-3	-2	-4	0	-8
Gapvd1	63 nt alt. 5'ss	-3	11	1	-10	-8	-6	-5	-6
Scrib	exon 84 nt	-9	15	2	2	1	-2	-2	-9
Trip10	exon 168 nt	-10	24	1	-1	4	-16	-8	-14
Fnbp1	exon 15 nt	-15	63	4	-5	-6	-10	-4	2
Ap2a1	exon 66 nt	-20	20	2	-2	-2	-7	-5	-4
Cltc	exon 21 nt	-25	14	-1	-5	-6	-8	-5	-7
Tmed2	exon 21 nt	-50	2	-6	-8	-8	-19	-17	-18
Capzb	exon 113 nt	-59	16	4	-9	-5	-7	-1	1

Δ PSI
-65 0 65

FIGURE 4. The expression of RBPs is regulated during myogenesis and influences splicing of membrane trafficking genes. (*A*) Quantification of RBP expression during myogenesis. Results are shown as mean ± SEM, $n = 6$, (*) $P < 0.05$, Welch's *t*-test. (*B–I*) PTBP1 (*B*), PTBP2 (*C*), RBFOX2 (*D*), QKI (*E*), CELF1 (*F*), CELF2 (*G*), MBNL1 (*H*), and MBNL2 (*I*) expression in myoblasts (Mb) and myotubes (Mt) was measured by western blotting. (*J*) Heatmap of splicing changes in trafficking genes upon RBP knockdown that were evaluated by RT-PCR assays and quantified by densitometry. ΔPSI was defined as the difference between the PSI in the knockdowns and the PSI in the control si-RNA. $n = 3$. (PSI) Percent spliced in.

PTBP1 and QKI co-regulate alternative splicing decisions in membrane trafficking genes

To determine the impact of our candidate RBPs on the expression of the muscle-specific isoforms of the membrane trafficking proteins under study, we depleted each RBP in C2C12 cells. In these experiments, undifferentiated cells were treated with small interfering RNAs (si-RNAs) and splicing outputs were evaluated after differentiation by RT-PCR assays. The exceptions to this approach were PTBP1, PTBP2, and RBFOX2. In PTBP1 and PTBP2 depletion experiments, splicing patterns were evaluated in undifferentiated cells because these RBPs are very lowly expressed in myotubes (Fig. 4B,C). On the other hand, RBFOX2 has a strong effect on C2C12 cell differentiation, especially in early stages (Singh et al. 2014). To avoid changes in alternative splicing that result from differentiation defects, myoblasts were differentiated for 2 d before transfection of RBFOX2 si-RNAs and then splicing outputs were evaluated 2 d later.

We observed relatively little effect of CELF1, CELF2, MBNL1, MBNL2, PTBP2, and RBFOX2 depletion on the splicing patterns of the selected membrane trafficking genes (Fig. 4J; Supplemental Figs. S5–S7). In contrast, PTBP1 and QKI depletion produced widespread changes in isoform expression of the trafficking genes (Fig. 4J; Supplemental Fig. S8). Depletion of PTBP1 in myoblasts (Fig. 5A) led to an increase in exon inclusion of 5% or more in 10 out of the 11 evaluated events (Fig. 4J; Supplemental Fig. S8A), including Fbln2 (Fig. 5B) and Capzb pre-mRNAs (Fig. 5C). No compensatory up-regulation in PTBP2 was observed following PTBP1 knockdown (Fig. 5A). QKI depleted myotubes (Fig. 5D) displayed an increase in exon inclusion for three events, such as those in Fbln2 (Fig. 5E) and Clta pre-mRNAs (Fig. 4J; Supplemental Fig. S8B), and increase in exon skipping for seven others, including Capzb (Fig. 5F), Fnbp1, Ap2a1, Cltc, and Tmed2 pre-mRNAs (Fig. 4J; Supplemental Fig. S8B).

Interestingly, PTBP1 and QKI appear to regulate the splicing of several events (Fbln2, Clta, Gapvd1 63 nt alt. 5′ss) in a cooperative manner, but others (Capzb, Cltc, Ap2a1, Fnbp1, Trip10, Scrib) in an antagonistic manner. These data indicate that the combined actions of PTBP1 and QKI determine splicing decisions in membrane trafficking genes during myogenesis.

In light of our discovery that QKI and PTBP1 coordinate the splicing of membrane trafficking genes, we examined the expression of RBPs in response to TSA or CPT treatment by western blotting (Supplemental Fig. S9A,B). Densitometry analysis revealed changes in expression of multiple RBPs following TSA or CPT treatment (Supplemental Fig. S9C–E). We were particularly interested in the protein expression changes of QKI and PTBP1 because they are major splicing regulators of membrane trafficking genes (Fig. 4J). To examine whether TSA and CPT may influence the splicing by altering RBP expression, we correlated the splicing results from TSA or CPT treatment with those from QKI or PTBP1 depletion (Supplemental Fig. S9F–H). We observed a strong correlation between splicing changes in response to TSA or CPT treatment and QKI depletion (Supplemental Fig. S9F–H, left) but not with PTBP1 depletion (Supplemental Fig. S9F–H, right). These results imply that TSA and CPT treatment may change splicing decisions in membrane trafficking genes by altering QKI expression.

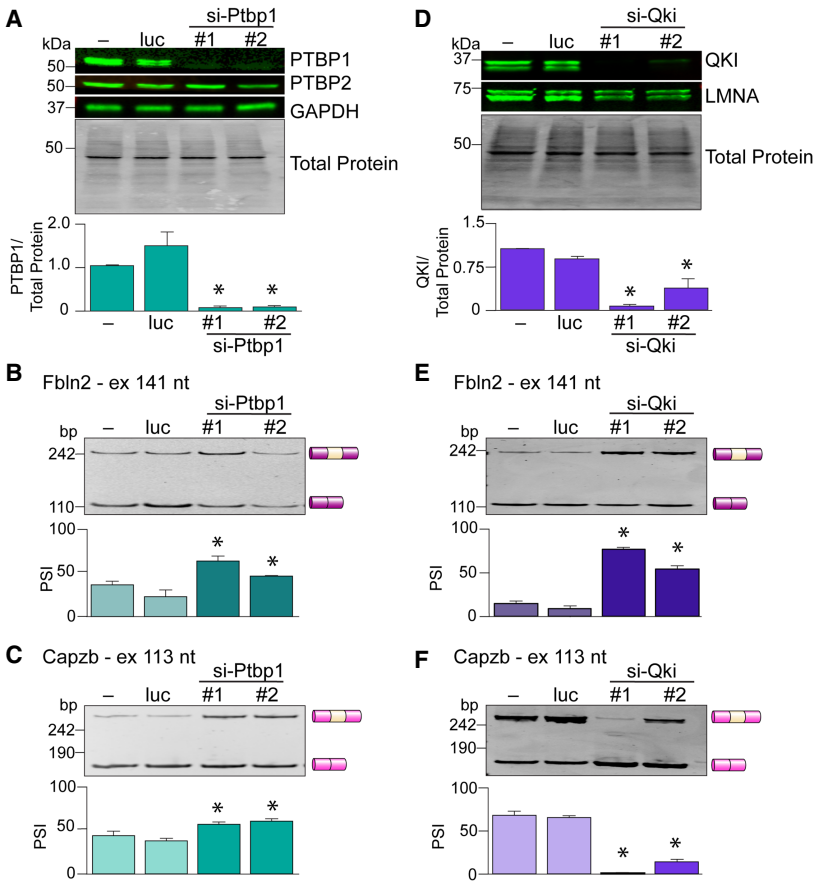

FIGURE 5. PTBP1 and QKI regulate alternative splicing in membrane trafficking genes. (*A*) PTBP1 was depleted in myoblasts, and western blot assays for PTBP1 and PTBP2 were performed (*top*), and the PTBP1 blot was quantified (*bottom*). (*B*,*C*) Splicing of several trafficking genes upon PTBP1 knockdown was evaluated by RT-PCR and quantified by densitometry. (*D*) QKI was depleted in myotubes, and western blot assays were performed (*top*) and quantified (*bottom*). (*E*,*F*) Splicing of several trafficking genes upon QKI depletion was evaluated by RT-PCR and quantified by densitometry. Results are shown as mean ± SEM, $n = 3$, (*) $P < 0.05$, Welch's *t*-test. (bp) Basepair, (KDa) kilodalton, (LMNA) lamin A/C, (nt) nucleotide.

Distribution of PTBP1 and QKI binding motifs around the alternative exons of membrane trafficking genes

We next asked whether there were putative PTBP1 and QKI binding motifs within the alternative exons or the flanking introns of our group of membrane trafficking genes. PTBP1 binds UCUCU motifs, particularly those upstream of alternatively spliced exons to induce exon skipping (Fig. 6A; Spellman and Smith 2006; Keppedipola 2012). In contrast, QKI is known to bind to ACUAA motifs upstream or downstream of an alternative exon to promote its skipping or inclusion, respectively (Fig. 6B; Galarneau and Richard 2005; Hall et al. 2013).

We utilized a set of ten 5-mer PTBP3 motifs (PTBP1 and PTBP3 share overlapping specificity) (Dominguez et al. 2018; Van Nostrand et al. 2020) and ten QKI motifs (Ray et al. 2013). By analyzing the alternative regions of the selected trafficking genes and up to 500 nt of the flanking intronic regions, we evaluated the presence and distribution of PTBP1 and QKI binding motifs. There were more PTBP1 motifs upstream of all alternatively spliced regions with some motifs downstream as well (Fig. 6C). This analysis, combined with our cell culture studies suggests that PTBP1 might bind upstream of alternative exons in membrane trafficking genes to promote exon skipping in myoblasts.

A higher number of QKI motifs were located upstream of alternative exons in *Fbln2*, *Trip10*, and *Clta* genes than downstream (Fig. 6D). Because QKI depletion led to an increase in inclusion of alternative exons in *Fbln2* and *Clta*, we propose that QKI might bind to the motifs located upstream of the alternative exons, thus acting as a negative splicing regulator for these splicing events. The regions downstream of the alternative exons in *Tmed2*, *Fnbp1*, *Cltc*, *Capzb*, and *Ap2a1* genes contained more QKI motifs than the upstream regions (Fig. 6D). When QKI was depleted, we observed an increase in exon skipping in *Tmed2*, *Fnbp1*, *Cltc*, *Capzb*, and *Ap2a1* genes, suggesting that QKI might bind to downstream motifs in these pre-mRNAs and act as a positive splicing regulator.

Overall, these findings suggest that membrane trafficking genes are regulated by alternative splicing by PTBP1 and QKI. PTBP1 acts as a splicing repressor by binding to upstream motifs, and QKI acts as a splicing silencer or enhancer when bound upstream or downstream of the alternative exon, respectively.

PTBP1 and RBFOX2 binding motifs are enriched around the entire set of alternative exons regulated during myogenesis

We used the previously mentioned RNA-sequencing data (Singh et al. 2014) to determine whether or not the distribution of motifs on trafficking genes are similar (or not) to all exons that are alternatively spliced during myogenesis. To determine motif enrichment, we performed an unbiased analysis of the 658 cassette exon events that change during myogenesis (427 events with $\Delta PSI \geq 0.1$ and 231 events with $\Delta PSI \leq -0.1$) and 658 unchanged cassette exon events matched based on length and GC-content.

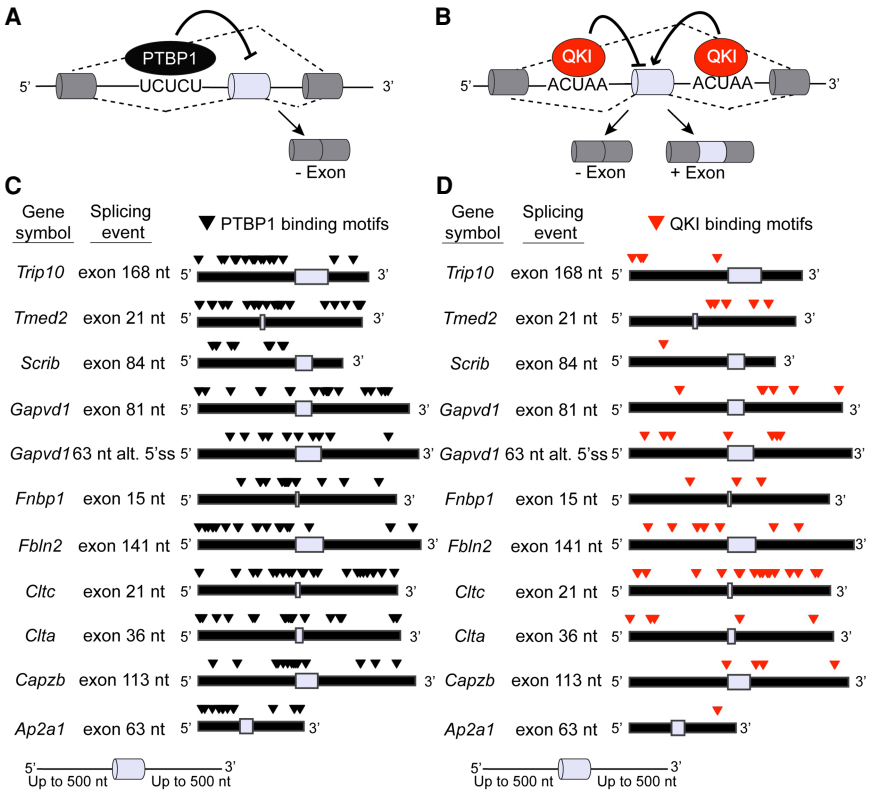

FIGURE 6. Membrane trafficking genes contain putative PTBP1 and QKI binding motifs in and around the alternatively spliced regions. (*A*,*B*) Schematic of the mechanism of PTBP1 (*A*) and QKI (*B*) regulation of alternative splicing. (*C*,*D*) Bioinformatic motif analysis for membrane trafficking genes for PTBP1 (*C*) and QKI (*D*). PTBP1 motifs are indicated by black triangles and QKI motifs by red triangles. Analysis was performed using ten PTBP1 motifs and ten QKI motifs. Exons and introns are scaled according to size. Up to 500 nt of the upstream intron and downstream intron was used for analysis.

Analysis of the alternative exon sequences revealed few enriched motifs (data not shown). However, investigation of intron sequences upstream of exons with positive ΔPSI values (ΔPSI ≥ 0.1, i.e., $PSI_{myotubes} > PSI_{myoblasts}$), revealed a significant enrichment of UC-rich motifs (Supplemental Fig. S10A, right). We did not observe a significant enrichment of UC-rich motifs for the upstream introns of alternative exons with negative ΔPSI values (ΔPSI ≤ −0.1, i.e., $PSI_{myoblasts} > PSI_{myotubes}$) (Supplemental Fig. S10A, left). The presence of UC-rich binding motifs upstream of differentially spliced exons suggests that PTBP1 might be a global splicing regulator during myogenesis.

Within the introns downstream of alternative exons regulated during myogenesis, we observed a significant enrichment of the RBFOX2 canonical motif, GCAUG, for events with positive ΔPSI values (Supplemental Fig. S10B, right). This is consistent with the finding that RBFOX2 promotes exon inclusion when binding downstream of the alternative exon (Sun et al. 2012). Interestingly, we did not observe an enrichment of QKI motifs in either the upstream or downstream introns of the exons undergoing alternative splicing during myogenesis, indicating that QKI regulation might be specific to particular splicing events, including membrane trafficking genes (Figs. 4J, 5D; Supplemental Fig. S10B).

Deletion of UCUCU motifs in Capzb and Fnbp1 pre-mRNAs prevents PTBP1 binding

To determine if the putative PTBP1 motifs identified by our bioinformatic analysis were occupied by this RBP, we performed in vitro binding assays. We first used fluorescence polarization experiments to assess PTBP1 binding affinity for RNA regions in the two events, *Capzb* and *Fnbp1*. RNA oligonucleotides (14–17 nt) containing consensus PTBP1 binding sequences mapping to either the alternative exon or the upstream flanking intron for *Capzb* (Fig. 7A) and *Fnbp1* (Fig. 7B) were synthesized. *Capzb* and *Fnbp1* gene sequences that did not have PTBP1 motifs were used as controls. We observed sigmoidal binding curves for the exon and intron oligonucleotides for both genes, with binding constants indicative of high-affinity binding similar to previous reports (Fig. 7C,D; Han et al. 2014). Importantly, control RNA sequences lacking PTBP1 motifs, or a randomized RNA sequence displayed substantially weaker or no binding (Fig. 7C,D, gray curves).

To corroborate our fluorescence polarization results we sought to assess PTBP1 binding to longer natural sequences (>100 nt) from *Capzb*. We adapted a previous method (Lambert et al. 2014; Dominguez et al. 2018) in which protein is immobilized to beads, incubated with RNA, and RNA binding is measured (in this case RNA binding is quantified by qPCR). Sequences spanning the *Capzb* intron or exon were in vitro transcribed to contain 5–6 PTBP1 motifs. As additional controls, we generated variants of Capzb RNAs in which PTBP1 motifs were mutated (C to G transitions, Fig. 7E, indicated as red circles) as well as a completely randomized RNA sequence which served as "background" binding (Fig. 7E–F). PTBP1 exhibited substantial binding to the wild-type *Capzb* intron sequence, which was greatly diminished with the RNAs harboring mutant motifs (Fig. 7G, left). PTBP1 association with the wild-type *Capzb* exon sequence was considerably weaker than with the intronic sequence (Fig. 7G), similar to our fluorescence polarization data (Fig. 7B), and also consistent with the preferred binding location of the protein in vivo.

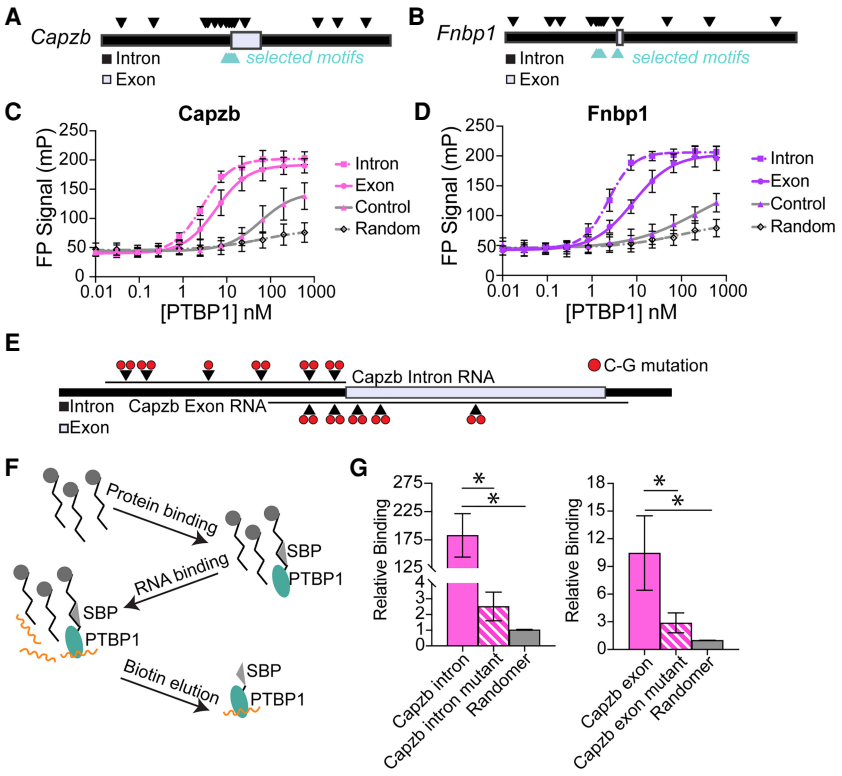

FIGURE 7. PTBP1 binds with high affinity to *Capzb* and *Fnbp1* intronic motifs in vitro. (*A*) Fluorescently labeled Capzb RNA oligonucleotides overlapping selected, putative PTBP1 binding motifs (arrowheads) identified within the alternative exon and up to 500 nt of flanking intron. (*B*) Fluorescently labeled Fnbp1 RNA oligonucleotides overlapping selected, putative PTBP1 binding motifs (arrowheads) identified within the alternative exon and up to 500 nt of the flanking introns. (*C*) Fluorescence polarization binding curves for Capzb RNA oligonucleotides incubated with PTBP1. Intron $K_D \sim 3$ nM (SD = 0.2 nM), exon $K_D \sim 6$ nM (SD = 2 nM). (*D*) Fluorescence polarization binding curves for Fnbp1 RNA oligonucleotides incubated with PTBP1. Intron $K_D \sim 2$ nM (SD = 0.9 nM), exon $K_D \sim 8$ nM (SD = 6 nM). (*E*) Capzb RNA oligonucleotides with wild-type or mutant putative PTBP1 motifs. (*F*) Schematic of Bind-n-qPCR assay. (*G*) PTBP1 binding enrichment to Capzb RNA oligonucleotides shown in panel *E*. Fluorescence polarization shows cumulative data with three replicates ($n = 3$). qPCR binding assays show cumulative data of replicates ($n = 5$). Significance was determined via one-tailed *t*-test, (*) $P < 0.05$.

Collectively, our data confirms the UCUCU motif as the consensus PTBP1 binding sequence and illustrates that PTBP1 preferentially binds to upstream intronic motifs with exceptionally high affinity for *Capzb* and *Fnbp1*.

DISCUSSION

Membrane trafficking proteins are involved in signal transduction, maintenance of ion concentration, clathrin-mediated endocytosis, vesicle-mediated transport, and secretory pathways, which are all especially critical to striated muscle physiology. In this work, we describe a set of membrane trafficking genes that are alternatively spliced in a tissue- and developmental stage-specific manner. The alternative regions in these membrane trafficking genes are small, and several fit the definition of microexons (i.e., exons containing 3–30 nt) (Ustianenko et al. 2017). Recent work demonstrated that inclusion or skipping of microexons can drastically alter protein binding partners and catalytic activity of enzymes (Ustianenko et al. 2017). Microexon inclusion can remodel entire protein binding networks in neurons, and likely behave similarly in other tissues (Irimia et al. 2014). Moreover, the majority of the alternative exons in membrane trafficking genes contain a multiple of three nucleotides, which translates to an in-frame insertion in the final peptide sequence and suggests that these isoforms may have novel functions that specifically support muscle function.

The combined actions of PTBP1 and QKI regulate splicing of membrane trafficking genes during myogenesis

PTBP1 and QKI have been shown to control an overlapping set of 172 exons during muscle cell differentiation in a microarray study (Hall et al. 2013). In our work, we find that membrane trafficking genes represent a functionally linked subset of genes that are regulated specifically by PTBP1 and QKI. In contrast, RBFOX2, which is an established regulator of splicing during muscle cell differentiation (Singh et al. 2014), is not a primary splicing regulator of membrane trafficking genes. The lack of global enrichment of QKI motifs in alternatively spliced genes during myogenesis and the presence of these motifs proximal to the alternative regions of trafficking genes further suggests that QKI specializes in regulating particular splicing events, including those in membrane trafficking genes. In our study and in others, PTBP1 generally acts as a negative splicing factor (Boutz et al. 2007). The down-regulation of PTBP1 expression during myogenesis may therefore function to relieve repression of alternative exons and allow the specific regulatory action of QKI to dictate adult splice isoform expression of membrane trafficking genes (Boutz et al. 2007). The close proximity of PTBP1 and QKI motifs suggests that a reduction in PTBP1 could also alleviate competition for binding of pre-mRNAs by QKI in adult tissues. Cooperation of splicing by multiple RBPs has been extensively demonstrated in many tissues. Thus, it is plausible that different pairs of RBPs coregulate subsets

of trafficking genes providing fail-safe mechanisms to prevent mis-splicing (Dassi 2017).

PTBP1 and QKI are expressed in numerous tissues, yet unique splice isoforms of the membrane trafficking genes evaluated here are expressed mostly in striated muscle. This observation might be explained by the fact that PTBP1 expression is down-regulated during striated muscle development, but not during the development of other tissues (Zhang et al. 2009; Carithers et al. 2015; Uhlén et al. 2015). Particularly high expression levels of QKI in striated muscle tissues may also contribute to these patterns (Uhlén et al. 2015; Chen et al. 2021). Indeed, a recent cross-species comparison of alternative splicing patterns indicates that QKI motifs tend to be located downstream of developmentally regulated exons in heart and likely function to promote the expression of adult heart isoforms (Mazin et al. 2021).

Chromatin-modifying drugs alter RBP expression

The chromatin-modifying drugs TSA and CPT have been extensively utilized to study the relationship between chromatin states, transcriptional kinetics, and alternative splicing outcomes. Although a relationship between treatment with TSA and CPT and histone acetylation or transcription rate has previously been experimentally established, our results suggest that expression of specific RBPs is also affected by TSA and CPT. In our studies, treatment of myotubes with TSA or CPT led to the down-regulation of QKI and produced splicing changes that resembled those in QKI depleted myotubes. These results suggest that the splicing effects observed after TSA and CPT treatment might be due to reduced QKI expression. These findings are likely to apply to non-muscle contexts where changes in the expression of other RBPs could mediate the effects observed after TSA or CPT exposure. These discoveries warrant a reexamination of the utility of these compounds in studying the relationship between transcriptional dynamics and alternative splicing.

Implications for striated muscle diseases

Mis-splicing of membrane-related genes is functionally tied to features of muscular and cardiac diseases (Savkur et al. 2004; Fugier et al. 2011; Tang et al. 2012; Hong et al. 2014; Freyermuth et al. 2016; Moulay et al. 2020). For example, a reversion to the expression of the fetal splice isoform of BIN1 has been observed in several muscular diseases and results in disorganized T-tubules (Fugier et al. 2011; Böhm et al. 2013). Bin1 pre-mRNA splicing is regulated by MBNL1 and splicing correction restores muscle strength in human muscle cells (Fugier et al. 2011). Another example is clathrin, a well-known endocytosis mediator, which consists of clathrin heavy chains and light chains coded for by the *Cltc* and *Clta* genes, respectively. Mice lacking the alternative exon of CLTC exhibit increased skeletal muscle mass and larger myofibers, indicating that *Cltc* splicing is functionally relevant for muscle development (Blue et al. 2018). Further, forced alternative exon skipping in *Cltc* results in abnormal clathrin plaque formation, reduced muscle force generation, and disruptions in intracellular architecture, establishing a novel role for the alternative exon in Cltc pre-mRNA in muscle homeostasis (Moulay et al. 2020). Increased skipping of the alternative exon was also correlated with myotonic dystrophy severity (Moulay et al. 2020). Our observation that QKI and PTBP1 antagonistically regulate the alternative exon in Cltc pre-mRNA suggests an important but unstudied potential role of these proteins in the pathogenic mechanism of myotonic dystrophy.

Final remarks

Proper expression of membrane trafficking proteins is critical for functional skeletal and cardiac muscle. Our study implicates PTBP1 and QKI in the regulation of this membrane trafficking splicing network. Greater insight into the splicing regulators of trafficking proteins and the function of alternative isoforms has the potential to reveal novel details about the still uncertain etiologies and molecular mechanisms underlying numerous diseases in striated muscle.

MATERIALS AND METHODS

Animals and tissue isolation

The FVB/NJ (The Jackson Laboratory) mouse colony was maintained from breeding pairs. Adult (4–5 mo) and postnatal day 4.5 (p4.5) mice were euthanized by the isoflurane drop method followed by secondary euthanasia techniques, such as cervical dislocation (adult) or decapitation (p4.5). Tissues were excised, blotted dry, flash frozen in liquid nitrogen, and stored at −80°C until further use. Mouse handling techniques followed the NIH Guidelines for Use and Care of Laboratory Animals approved by the Institutional Animal Care and Use Committee (IACUC) at The University of North Carolina at Chapel Hill (UNC Chapel Hill).

Cell culture

C2C12 mouse myoblast cells (ATCC) were cultured at 37°C under 5% CO_2 in Dulbecco's Modified Eagle Medium (DMEM) supplemented with 10% fetal bovine serum (FBS), 2 mM glutamine, 100 units/mL of penicillin, and 100 µg/mL streptomycin. Cells were maintained at low confluency (30%–40% confluent). For differentiation, cells were washed with phosphate buffered saline (PBS) and cultured in DMEM supplemented with 2% horse serum, 2 mM glutamine, 100 units/mL of penicillin, and 100 µg/mL streptomycin. Differentiation media were replaced every 48 h.

si-RNA delivery

C2C12 myoblast cells were plated in six well plates (60–80 × 10^3 cells per well) in DMEM supplemented with 10% FBS and 2 mM glutamine. Delivery of si-PTBP1 (Invitrogen, MSS276537, MSS 276539), si-PTBP2 (Invitrogen, MSS225938, MSS225940), si-QKI (Invitrogen, MSS208338, MSS276677), si-MBNL1 (Invitrogen, MSS226392, MSS226393), si-MBNL2 (Invitrogen, MSS272396, MSS200587), si-CELF1 (Invitrogen, MSS203372, MSS203374), or si-CELF2 (Invitrogen, MSS274200, MSS204012) was performed the following day when the cells reached 50%–60% confluency using the Lipofectamine RNAiMax transfection reagent (Invitrogen, 13778075) following manufacturer protocols. Prior to transfection of si-RBFOX2 (Dharmacon, D-051552-01-0002, D-051552-04-0002), myoblasts were differentiated for 2 d. A si-luciferase (si-luc) (Invitrogen, 465377) was used as a negative control for experiments using the stealth si-RNAs from Invitrogen and a non-targeting si-RNA (Dharmacon, D-001210-01-20) was used as a negative control for experiments using the si-RNAs from Dharmacon. For PTBP1 and PTBP2 depletion experiments, cells were washed with PBS and RNA, and protein lysates were extracted 24 h after transfection. Cells were differentiated for 4–6 d before RNA and protein collection for QKI, MBNL1, MBNL2, CELF1, CELF2, and RBFOX2 depletion experiments.

TSA and CPT treatment

C2C12 myoblasts were plated in six well plates (200–300 × 10^3 cells per well) in DMEM supplemented with 10% FBS and 2 mM glutamine. Differentiation was initiated the following day by switching the culture medium to DMEM supplemented with 2% horse serum and 2 mM glutamine. After 3–6 d of differentiation, cells were treated with 1 µg/mL TSA, 1 µM CPT, 10 µM CPT, or an equal volume of dimethyl sufloxide (DMSO, vehicle) for 16–18 h.

RNA extraction

Flash frozen tissues were pulverized using 1.4 mm ceramic beads (Lysing Matrix D) and TRIzol Reagent (Invitrogen) at 6500 r.p.m. for 20 sec intervals using a Precellys-24 Homogenizer (Bertin Instruments). Total RNA was extracted following the TRIzol Reagent manufacturer's recommended protocol. Total RNA concentration was measured using a NanoDrop Lite Spectrophotometer (ND-LITE, Thermo Fisher Scientific).

cDNA synthesis

RNA was reverse-transcribed into cDNA using the High-Capacity cDNA Reverse Transcription Kit (Applied Biosystems, 4368813), nuclease-free water and RNase inhibitors (Applied Biosystems, N8080119), and the following program: (i) 25°C for 10 min, (ii) 37°C for 120 min, (iii) 85°C for 5 min, (iv) 4°C pause.

Alternative splicing evaluation by PCR

cDNA was utilized to perform PCR assays using GoTaq Green Master Mix (Promega, #M7123) and mouse primers (0.5 µM) that targeted the constitutive exons that flank the alternative spliced regions (Supplemental Table S1). Amplification conditions were as follows: (i) 95°C for 1 min 15 sec, (ii) 28 cycles of 95°C for 45 sec, 57°C for 45 sec, 72°C for 1 min, (iii) 72°C for 10 min, (iv) 4°C pause. PCR products were separated by electrophoresis using 6% polyacrylamide gels in TBE buffer (89 mM Tris, 89 mM boric acid, 2.5 mM EDTA, pH 8.3) for 4 h at 140 V. Gels were stained with an aqueous solution of 0.4 µg/mL ethidium bromide for 10 min and visualized using the ChemiDoc XRS+ Imaging System (Bio-Rad). The Image Lab 6.0.1 Software (Bio-Rad) for analysis was utilized to quantify the alternative splicing gels by densitometry.

Quantitative real-time PCR (qPCR)

Applied Biosystems TaqMan Fast Advanced Master Mix (Thermo Fisher Scientific, #4444557) was used in 20 µL reaction with 25 ng cDNA. The following protocol was run on a StepOne Plus Machine: (i) 50°C for 2 min; (ii) 95°C for 20 sec; (iii) 95°C for 1 sec; (iv) 60°C for 20 sec. The cycle thresholds for all probes were normalized to ribosomal protein L13a (Rpl13a, Mm01612986_gH, amplicon size 122 bp; Thermo Fisher Scientific) (Supplemental Table S2).

Protein lysate preparation

Cells were placed on ice, washed with ice cold PBS, and lysed on ice with cold RIPA lysis buffer (50 mM Tris, 150 mM NaCl, 1% Triton X-100, 0.5% sodium deoxycholate, 0.1% sodium dodecyl sulfate [SDS], pH 7.5) containing protease inhibitors (Roche, 11873580001, 04693132001) and phosphatase inhibitors (Thermo Fisher Scientific, #78428), and 1 mM EDTA. Lysates were incubated on ice for 15 min, sonicated at 75% amplitude for 3 min (30 sec on, 30 sec off), incubated on ice for 15 min and then centrifuged at 14,000 r.p.m. for 10 min at 4°C. Supernatants were transferred into new tubes and stored at −80°C. Protein concentration was measured using the Pierce BCA Protein Assay Kit (Thermo Fisher Scientific, #23225).

Western blotting

Equal amounts of protein were diluted in loading buffer (50 mM Tris-HCl pH 6.8, 12.5 mM EDTA, 10% glycerol, 2% SDS, 0.02% bromophenol blue, 360 mM beta-mercaptoethanol). Samples were analyzed by SDS polyacrylamide gel electrophoresis (SDS-PAGE) on TGX-stain-free gels (Bio-Rad) utilizing a buffer containing 192 mM glycine, 25 mM Tris-base, and 3.5 mM SDS, pH 8.3. Electrophoresis was performed at 90 V for 30 min and 90–150 V for 30 min. Gels were imaged on a ChemiDoc XRS+ Imaging System (Bio-Rad). Proteins were then transferred into an Amersham Hybond Low Fluorescence 0.2 µm PVDF membrane (General Electric Healthcare, #10600022) at 100 V for 1 h using a transfer buffer, which contains 192 mM glycine, 25 mM Tris, and 20% methanol, pH 8.3. Membranes were imaged on a ChemiDoc Imaging System (Bio-Rad) to estimate total protein in each lane. Membranes were then blocked for 1 h at room temperature using 5% nonfat dry milk in tris-buffered saline with tween (TBST) (20 mM Tris-base, 137 mM NaCl, 0.1% tween 20, pH 7.6). Membranes were washed

briefly with TBST and then incubated overnight at 4°C with the appropriate primary antibodies diluted in 1% BSA in TBST. Primary antibodies and the utilized dilutions were as follows: anti-PTBP1 from Abcam (ab133734,1:5,000 or 1:10,000), anti-PTBP2 from Abcam (ab154787,1:5,000 or 1:2,000), anti-RBFOX2 from Santa Cruz Biotechnology (sc271407,1:500), anti-QKI from Abcam (ab126742,1:1,000), anti-MBNL1 from Santa Cruz Biotechnology (sc515374,1:250), anti-MBNL2 from Santa Cruz Biotechnology (sc136167,1:200 or 1:500), anti-CELF1 from Santa Cruz Biotechnology (sc20003,1:200 or 1:1,000), anti-CELF2 from Santa Cruz Biotechnology (sc47731,1:200), anti-glyceraldehyde-3-phosphate dehydrogenase (GAPDH) from Santa Cruz Biotechnology (sc365062,1:100), anti-lamin A/C from Santa Cruz Biotechnology (sc7293,1:500), anti-vinculin (VCL) from Cell Signaling Technology (#4650,1:1,000), anti-acetyl-histone H3 (H3ac) from Millipore (#06-599,1:500). The following day, membranes were washed in TBST three times (10 min each) and incubated with the appropriate secondary antibodies diluted (1:10,000) in 1% BSA in TBST for 1–1.5 h in darkness and at room temperature. Secondary antibodies utilized were purchased from Thermo Fisher Scientific and were as follows: anti-mouse Dylight 800 (SA5-35521) and anti-rabbit Dylight 800 (SA5-35571). Membranes were imaged using an Odyssey Licor Imager.

Unbiased motif analysis

RNA-sequencing data from one sample of undifferentiated C2C12 myoblasts and two samples of differentiated C2C12 myotubes were utilized (Singh et al. 2014). Samples were aligned to the mm10 genome using STAR (Dobin et al. 2013), then sorted and indexed using bedtools (Quinlan and Hall 2010), and alternative splicing was calculated using MISO (Katz et al. 2010) (undifferentiated sample compared to the two differentiated samples). Cassette exon events from the two MISO comparisons were combined. Significant events were defined as those with a Bayes factor ≥ 10 and $\Delta PSI \geq 0.1$ (positive ΔPSI) or Bayes factor ≥ 10 and $\Delta PSI \leq -0.1$ (negative ΔPSI). Length and GC content were calculated for the alternatively spliced exons, and the upstream and downstream flanking introns (up to 500 bp). Sequences with similar length and GC content within each of those subcategories were matched using the MatchIt R package to generate a control set (Ho et al. 2011). 5-mer frequency was computed for these regions, and the frequency of 5-mers in significant events compared to matched control nonsignificant events was calculated using a Fisher's exact test. Significant 5-mers with a $P_{adj} < 0.05$ were plotted. For both cases, ΔPSI was defined as the difference between the PSI in myotubes and the PSI in myoblasts ($\Delta PSI = PSI_{myotubes} - PSI_{myoblasts}$). Using these sets of exons, upstream and downstream introns of the exons were determined.

Biased motif analysis

By utilizing a set of ten 5-mer PTBP3 motifs (TTTCT, TCTTT, TCTCT, TTCTT, CTATC, CTTTC, TCTAT, CTTCT, TATCT, CTTTT) in vitro specificity of the RBP was determined (Dominguez et al. 2018). For QKI, a set of ten 5-mer QKI motifs identified in vitro were utilized (ACTAA, CTAAC, CTAAT, TACTA, CTAAC, TCTAA, CTAAG, GACTA, AACTA, CTGTA) (Ray et al. 2013). Using those motifs, the alternative exons of the 11 events in the trafficking genes and up to 500 nt of the upstream and downstream introns were analyzed to determine the presence and location of PTBP1 and QKI binding motifs.

GO analysis

GO enrichment analysis was performed using ClusterProfiler (Yu et al. 2012). A background set of genes expressed during C2C12 cell differentiation was used to compare with the cassette exon events considered differentially spliced according to the criteria described above. The −log10 value was calculated from the Benjamini–Hochberg adjusted *P*-value outputted from Cell Profiler.

Analysis of splice site strength

Sequences were retrieved from Ensembl genome browser. Splice site strength was calculated using MaxEntScan::score5ss and MaxEntScan::score3ss (Yeo and Burge 2004). The strength of the 5′ splice site was defined as the mean scores determined by the maximum entropy model, maximum dependence decomposition model, first-order Markov model, and weight matrix model. The strength of the 3′ splice site was defined as the mean scores determined by the maximum entropy model, first-order Markov model, and weight matrix model. A cutoff of 10% was used to define alternative sites that were higher or lower than the constitutive sites.

Expression and purification of PTBP1

PTBP1 isoform 1 was cloned out of pGEX-2TK-PTB from Phil Sharp (Garcia-Blanco et al. 1989) (Addgene, plasmid #21929; http://n2t.net/addgene:21929; RRID:Addgene_21929)1, cloned into a pGEX-6P-1 construct containing GST and SBP (streptavidin binding peptide) tags, and transformed into BL21(DE3) *E. coli* cells. Cultures were grown in LB media until an optical density of ∼0.8 was reached, the temperature was adjusted to 16°C and the cultures were induced with 0.5 mM IPTG (Thermo Fisher Scientific) overnight. Cells were collected by centrifugation at 4000*g* for 15 min and lysed in a buffer containing 50 mM Tris pH 7.6, 200 mM NaCl, 5 mM DTT, 500 units/L culture Benzonase Nuclease (Sigma-Aldrich), and 2 mM phenylmethylsulfonyl fluoride (PMSF). Lysates were sonicated and centrifuged at 36,000*g* for 30 min. Supernatants were then passed over a 0.45 μm filter. GST-SBP-PTBP1 was purified using GST-trap FF columns (General Electric Healthcare). Protein concentration was determined via Pierce 660 nm assay (Thermo Fisher Scientific), and purity was assessed via SDS-PAGE and Coomassie blue staining.

In vitro transcription of RNA oligonucleotides

Intron and exon DNA oligonucleotides for Capzb were ordered from Integrated DNA Technologies (IDT) and PCR amplified using FWD_adapter and REV_adapter primers (Supplemental Table S3) from IDT to produce the full-length DNA oligonucleotides with qPCR adapters and a T7 promoter. DNA was resolved via agarose gel electrophoresis and the resultant bands were extracted utilizing a QIAquick Gel Extraction Kit (Qiagen). DNA was in vitro transcribed using a T7 RiboMAX Express Large Scale RNA Production System (Promega) to produce final RNA oligos with qPCR adapters

(Supplemental Table S3). Final purity was assessed via denaturing acrylamide gel electrophoresis, and RNA concentration was determined using a NanoDrop One (Thermo Fisher Scientific).

qPCR binding assay

Dynabeads MyOne Streptavidin T1 (Thermo Fisher Scientific) were washed first with nuclease-free water, then blocking buffer containing 25 mM Tris pH 8.0, 150 mM KCl, 3 mM $MgCl_2$, 1 mg/mL BSA, 2 units/µL SUPERase-In (Invitrogen), and 1 mg/mL yeast tRNA (Thermo Fisher Scientific), and finally with binding buffer (25 mM Tris pH 8.0, 150 mM KCl, 3 mM $MgCl_2$, 1 mg/mL BSA, 2 units/mL SUPERase-In, and 50 nM random 14 nt RNA oligo). Reactions were assembled in triplicate with 20 µL of beads, 50 nM GST-SBP-PTBP1, and 5 nM transcribed RNA and diluted to a final volume of 60 µL in binding buffer. Reactions were left to equilibrate for 30 min at 25°C. Following equilibration, the reactions were placed on a magnetic stand for 2 min to isolate the PTBP1–RNA complexes. Unbound RNA was removed, and the beads were washed three times with 180 µL of wash buffer (25 mM Tris pH 8.0, 150 mM KCl, 2 mM $MgCl_2$, 2 units/mL SUPERase-In, and 50 nM random sequence RNA). Product reactions were washed for 5 min and then placed on the magnet. PTBP1–RNA complexes were eluted from the magnetic beads in elution buffer (4 mM biotin, 25 mM Tris pH 8.0) for 30 min at 37°C. The product reactions were placed back on the magnetic stand and the PTBP1–RNA complexes were collected. Collected RNA was reverse transcribed using the iScript Reverse Transcription Supermix (Bio-Rad) following manufacturer's protocol with RT primer (5′-CGT-TGA-CAC-TCG-ACG-ACT-GCA-3′) from IDT. Total input RNA (0.3 pmol) was reverse transcribed to allow for RNA input normalization following qPCR. Template cDNA from RT was amplified by qPCR utilizing the SsoAdvanced Universal SYBR Green Supermix (Bio-Rad) according to manufacturer's instructions with qPCR_FWD primer (5′-AGT-TGT-ACA-GTC-CGA-CGA-TGC-3′) and qPCR_REV primer (5′-CGT-TGA-CAC-TCG-ACG-ACT-GCA-3′), both from IDT. The threshold cycle (C_t) was determined for each, and ΔC_t values were used to quantify the binding differences between wild-type and mutant oligonucleotides. All values were normalized to the C_t values of the input RNA and randomer ΔC_t values.

Fluorescence polarization assay

RNA oligonucleotides with a 6-FAM (fluorescein) label at the 3′ end were purchased from IDT and their sequences are as follows: Capzb intron (5′-CUC-UCU-GAA-CAC-UCU-CU-/6-FAM/-3′), Capzb exon (5′-AUC-UCU-UGA-UGC-UAU-CC-/6-FAM/-3′), Capzb control (5′-AGC-GCC-AGG-UCU-AC-/6-FAM/-3′), Fnbp1 intron (5′-CUC-UCU-CUC-UCU-CUC-UC-/6-FAM/-3′), Fnbp1 exon (5′-CUU-UCU-CUC-AAG-CU-/6-FAM/-3′), Fnbp1 control (5′-CUG-GUC-UAA-UUG-GGU-UC-/6-FAM/-3′). GST-SBP-PTBP1 was serial diluted in FP binding buffer [20 mM HEPES, 50 mM $NaC_2H_3O_2$, 3 mM $Mg(C_2H_3O_2)_2$, 0.01% triton X-100, 5 mM GSH, and 10 µg/mL BSA, pH 6.5] at the indicated final concentrations. RNA (to 5 nM final) was added and the reactions were incubated for 15 min at 4°C. Plates were then centrifuged at 1000*g* for 1 min. Fluorescence polarization was measured at 25°C using a PHERAstar Plate Reader (BMG Labtech). Data were fit to a four-parameter logistic regression and a K_d was determined.

Statistical analysis

Significance was determined using an unpaired Welch's *t*-test (two-tailed). When multiple groups were compared, a one-way ANOVA with Bonferroni post-hoc test for multiple comparisons was applied to test significance. For RNA-sequencing analysis, adjusted *P*-value ($P_{adjusted}$) was used to account for multiple comparisons. qPCR binding significance was determined via *t*-test. Statistical analysis was performed in Microsoft Excel (Microsoft), RStudio or in Prism 9 (GraphPad). Statistical significance was considered if $P < 0.05$ or $P_{adjusted} < 0.05$. All data are represented as mean ± SEM.

SUPPLEMENTAL MATERIAL

Supplemental material is available for this article.

ACKNOWLEDGMENTS

This work was supported by start-up funds (J.G. and D.D.) and a Jefferson Pilot Award (J.G.) from The University of North Carolina at Chapel Hill, the National Institutes of Health (NIH-NIGMS R01GM130866), (J.G.) and a Career Development Award from the American Heart Association (19CDA34660248) (J.G.). E. R.H was supported by a NIH-NIAMS F31 predoctoral fellowship (AR077381-01A1) and a NIH-NIGMS training award (5T32GM007092). H.J.W. was supported by a merit-doctoral fellowship from the Graduate School at The University of North Carolina at Chapel Hill, a NIH-NIGMS training award (T32GM119999), and by the NSF Graduate Research Fellowship Program (DGE-1650116). G.M.G. was supported by a NIH-NIGMS training award (T32GM119999) and by the NSF Graduate Research Fellowship Program (DGE-1650116). E.V.T. was supported by the Chancellor's Science Scholars Program at the University of North Carolina at Chapel Hill. A.J.B. was supported by a NIH-NHLBI F32 postdoctoral fellowship (F32HL149147). S.E.H. was supported by a NIH-NIGMS training award (T32GM008570). B.B.G. was supported by NIH-NIGMS training awards T32GM135095 and R25GM055336. We acknowledge the support of the Genetics and Molecular Biology Curriculum (GMB), the Program in Translational Medicine, and the Mechanistic and Interdisciplinary Biology (MiBio) Graduate Training Program, all at The University of North Carolina at Chapel Hill. The content is solely the responsibility of the authors and does not necessarily represent the official views of the National Institutes of Health or the other funding agencies.

Author contributions: E.R.H., H.J.W., E.V.T., M.J., A.J.B., R.E.B., S.H.E., B.B.G., G.M.G., E.Y.L., and J.G. performed experiments. E.R.H., H.J.W., A.J.B., R.E.B., S.H.E., B.B.G., G.M.G., E.Y.L., D.D., and J.G. analyzed the data. E.R.H. performed the bioinformatics analysis. Y.-H.T., J.P., and D.D. contributed with bioinformatics knowledge, tools, and supervision. E.R.H., H.J.W., and J.G. wrote the draft, and all authors edited and approved the final manuscript. J.G. conceived and supervised the study.

Received September 27, 2021; accepted December 17, 2021.

REFERENCES

Agirre E, Oldfield AJ, Bellora N, Segelle A, Luco RF. 2021. Splicing-associated chromatin signatures: a combinatorial and position-

dependent role for histone marks in splicing definition. *Nat Commun* **12:** 1–16. doi:10.1038/s41467-021-20979-x

Alexander RD, Innocente SA, Barrass JD, Beggs JD. 2010. Splicing-dependent RNA polymerase pausing in yeast. *Mol Cell* **40:** 582–593. doi:10.1016/j.molcel.2010.11.005

Al-Qusairi L, Laporte J. 2011. T-tubule biogenesis and triad formation in skeletal muscle and implication in human diseases. *Skelet Muscle* **1:** 26. doi:10.1186/2044-5040-1-26

Ames EG, Lawson MJ, Mackey AJ, Holmes JW. 2013. Sequencing of mRNA identifies re-expression of fetal splice variants in cardiac hypertrophy. *J Mol Cell Cardiol* **62:** 99–107. doi:10.1016/j.yjmcc.2013.05.004

Barr FA, Preisinger C, Kopajtich R, Körner R. 2001. Golgi matrix proteins interact with p24 cargo receptors and aid their efficient retention in the Golgi apparatus. *J Cell Biol* **155:** 885–891. doi:10.1083/jcb.200108102

Batra R, Charizanis K, Manchanda M, Mohan A, Li M, Finn DJ, Goodwin M, Zhang C, Sobczak K, Thornton CA, et al. 2014. Loss of MBNL leads to disruption of developmentally regulated alternative polyadenylation in RNA-mediated disease. *Mol Cell* **56:** 311–322. doi:10.1016/j.molcel.2014.08.027

Bintu L, Ishibashi T, Dangkulwanich M, Wu YY, Lubkowska L, Kashlev M, Bustamante C. 2012. Nucleosomal elements that control the topography of the barrier to transcription. *Cell* **151:** 738–749. doi:10.1016/j.cell.2012.10.009

Bland CS, Wang ET, Vu A, David MP, Castle JC, Johnson JM, Burge CB, Cooper TA. 2010. Global regulation of alternative splicing during myogenic differentiation. *Nucleic Acids Res* **38:** 7651–7664. doi:10.1093/nar/gkq614

Blue RE, Koushik A, Engels NM, Wiedner HJ, Cooper TA, Giudice J. 2018. Modulation of alternative splicing of trafficking genes by genome editing reveals functional consequences in muscle biology. *Int J Biochem Cell Biol* **105:** 134–143. doi:10.1016/j.biocel.2018.10.004

Böhm J, Vasli N, Maurer M, Cowling B, Shelton GD, Kress W, Toussaint A, Prokic I, Schara U, Anderson TJ, et al. 2013. Altered splicing of the BIN1 muscle-specific exon in humans and dogs with highly progressive centronuclear myopathy. *PLoS Genet* **9:** e1003430. doi:10.1371/journal.pgen.1003430

Boutz P, Chawla G. 2007. MicroRNAs regulate the expression of the alternative splicing factor nPTB during muscle development. *Genes Dev* **21:** 71–84. doi:10.1101/gad.1500707

Boutz PL, Stoilov P, Li Q, Lin CH, Chawla G, Ostrow K, Shiue L, Ares M, Black DL. 2007. A post-transcriptional regulatory switch in polypyrimidine tract-binding proteins reprograms alternative splicing in developing neurons. *Genes Dev* **21:** 1636–1652. doi:10.1101/gad.1558107

Brinegar AE, Xia Z, Loehr JA, Li W, Rodney GG, Cooper TA. 2017. Extensive alternative splicing transitions during postnatal skeletal muscle development are required for Ca^{2+} handling. *Elife* **6:** e27192. doi:10.7554/eLife.27192

Carithers LJ, Ardlie K, Barcus M, Branton PA, Britton A, Buia SA, Compton CC, Deluca DS, Peter-Demchok J, Gelfand ET, et al. 2015. A novel approach to high-quality postmortem tissue procurement: the GTEx project. *Biopreserv Biobank* **13:** 311–317. doi:10.1089/bio.2015.0032

Chen X, Liu Y, Xu C, Ba L, Liu Z, Li X, Huang J, Simpson E, Gao H, Cao D, et al. 2021. QKI is a critical pre-mRNA alternative splicing regulator of cardiac myofibrillogenesis and contractile function. *Nat Commun* **12:** 1–18. doi:10.1038/s41467-020-20314-w

Danan-Gotthold M, Golan-Gerstl R, Eisenberg E, Meir K, Karni R, Levanon EY. 2015. Identification of recurrent regulated alternative splicing events across human solid tumors. *Nucleic Acids Res* **43:** 5130–5144. doi:10.1093/nar/gkv210

Dassi E. 2017. Handshakes and fights: the regulatory interplay of RNA-binding proteins. *Front Mol Biosci* **4:** 1–8. doi:10.3389/fmolb.2017.00067

Dobin A, Davis CA, Schlesinger F, Drenkow J, Zaleski C, Jha S, Batut P, Chaisson M, Gingeras TR. 2013. STAR: ultrafast universal RNA-seq aligner. *Bioinformatics* **29:** 15–21. doi:10.1093/bioinformatics/bts635

Dominguez D, Freese P, Alexis MS, Su A, Hochman M, Palden T, Bazile C, Lambert NJ, Van Nostrand EL, Pratt GA, et al. 2018. Sequence, structure, and context preferences of human RNA binding proteins. *Mol Cell* **70:** 854–867. doi:10.1016/j.molcel.2018.05.001

Dowling JJ, Gibbs EM, Feldman EL. 2008. Membrane traffic and muscle: lessons from human disease. *Traffic* **9:** 1035–1043. doi:10.1111/j.1600-0854.2008.00716.x

Du H, Cline MS, Osborne RJ, Tuttle DL, Clark TA, Donohue JP, Hall MP, Shiue L, Swanson MS, Thornton CA, et al. 2010. Aberrant alternative splicing and extracellular matrix gene expression in mouse models of myotonic dystrophy. *Nat Struct Mol Biol* **17:** 187–193. doi:10.1038/nsmb.1720

Dujardin G, Lafaille C, de la Mata M, Marasco LE, Muñoz MJ, Le Jossic-Corcos C, Corcos L, Kornblihtt AR. 2014. How slow RNA polymerase II elongation favors alternative exon skipping. *Mol Cell* **54:** 683–690. doi:10.1016/j.molcel.2014.03.044

Franzini-Armstrong C. 1991. Simultaneous maturation of transverse tubules and sarcoplasmic reticulum during muscle differentiation in the mouse. *Dev Biol* **146:** 353–363. doi:10.1016/0012-1606(91)90237-W

Freyermuth F, Rau F, Kokunai Y, Linke T, Sellier C, Nakamori M, Kino Y, Arandel L, Jollet A, Thibault C, et al. 2016. Splicing misregulation of *SCN5A* contributes to cardiac-conduction delay and heart arrhythmia in myotonic dystrophy. *Nat Commun* **11:** 11067. doi:10.1038/ncomms11067

Fugier C, Klein AF, Hammer C, Vassilopoulos S, Ivarsson Y, Toussaint A, Tosch V, Vignaud A, Ferry A, Messaddeq N, et al. 2011. Misregulated alternative splicing of *BIN1* is associated with T tubule alterations and muscle weakness in myotonic dystrophy. *Nat Med* **17:** 720–725. doi:10.1038/nm.2374

Galarneau A, Richard S. 2005. Target RNA motif and target mRNAs of the quaking STAR protein. *Nat Struct Mol Biol* **12:** 691–698. doi:10.1038/nsmb963

Garcia-Blanco MA, Jamison SF, Sharp PA. 1989. Identification and purification of a 62,000-dalton protein that binds specifically to the polypyrimidine tract of introns. *Genes Dev* **3:** 1874–1886. doi:10.1101/gad.3.12a.1874

Giudice J, Cooper TA. 2014. RNA-binding proteins in heart development. In *Systems biology of RNA binding proteins* (ed. Yeo GW), pp. 389–429. Springer, NY

Giudice J, Xia Z, Wang ET, Scavuzzo MA, Ward AJ, Kalsotra A, Wang W, Wehrens XHT, Burge CB, Li W, et al. 2014. Alternative splicing regulates vesicular trafficking genes in cardiomyocytes during postnatal heart development. *Nat Commun* **5:** 3603. doi:10.1038/ncomms4603

Giudice J, Loehr JA, Rodney GG, Cooper TA. 2016. Alternative splicing of four trafficking genes regulates myofiber structure and skeletal muscle physiology. *Cell Rep* **17:** 1923–1933. doi:10.1016/j.celrep.2016.10.072

Gokhin DS, Ward SR, Bremner SN, Lieber RL. 2008. Quantitative analysis of neonatal skeletal muscle functional improvement in the mouse. *J Exp Biol* **211:** 837–843. doi:10.1242/jeb.014340

Hall MP, Nagel RJ, Fagg WS, Shiue L, Cline MS, Perriman RJ, Donohue JP, Ares M Jr. 2013. Quaking and PTB control overlapping splicing regulatory networks during muscle cell differentiation. *RNA* **19:** 627–638. doi:10.1261/rna.038422.113

Han A, Stoilov P, Linares AJ, Zhou Y, Fu XD, Black DL. 2014. *De novo* prediction of PTBP1 binding and splicing targets reveals unexpected features of its RNA recognition and function. *PLoS Comput Biol* **10:** e1003442. doi:10.1371/journal.pcbi.1003442

Ho DE, King G, Stuart EA, Imai K. 2011. MatchIt : nonparametric preprocessing for parametric causal inference. *J Stat Softw* **42:** 1–28. doi:10.18637/jss.v042.i08.

Hong T, Yang H, Zhang S-S, Cho HC, Kalashnikova M, Sun B, Zhang H, Bhargava A, Grabe M, Olgin J, et al. 2014. Cardiac BIN1 folds T-tubule membrane, controlling ion flux and limiting arrhythmia. *Nat Med* **20:** 624–632. doi:10.1038/nm.3543

Irimia M, Weatheritt RJ, Ellis JD, Parikshak NN, Gonatopoulos-Pournatzis T, Babor M, Quesnel-Vallières M, Tapial J, Raj B, O'Hanlon D, et al. 2014. A highly conserved program of neuronal microexons is misregulated in autistic brains. *Cell* **159:** 1511–1523. doi:10.1016/j.cell.2014.11.035

Kalsotra A, Xiao X, Ward AJ, Castle JC, Johnson JM, Burge CB, Cooper TA. 2008. A postnatal switch of CELF and MBNL proteins reprograms alternative splicing in the developing heart. *Proc Natl Acad Sci* **105:** 20333–20338. doi:10.1073/pnas.0809045105

Katz Y, Wang ET, Airoldi EM, Burge CB. 2010. Analysis and design of RNA sequencing experiments for identifying isoform regulation. *Nat Methods* **7:** 1009–1015. doi:10.1038/nmeth.1528

Keppedipola N. 2012. Neuronal regulation of pre-mRNA splicing by polypyrimidine tract binding proteins, PTB1 and PTB2. *Crit Rev Biochem Mol Biol* **47:** 360–378. doi:10.3109/10409238.2012.691456

Khan DH, Gonzalez C, Cooper C, Sun JM, Chen HY, Healy S, Xu W, Smith KT, Workman JL, Leygue E, et al. 2014. RNA-dependent dynamic histone acetylation regulates *MCL1* alternative splicing. *Nucleic Acids Res* **42:** 1656–1670. doi:10.1093/nar/gkt1134

Lambert N, Robertson A, Jangi M, McGeary S, Sharp PA, Burge CB. 2014. RNA Bind-n-Seq: quantitative assessment of the sequence and structural binding specificity of RNA binding proteins. *Mol Cell* **54:** 887–900. doi:10.1016/j.molcel.2014.04.016

Listerman I, Sapra AK, Neugebauer KM. 2006. Cotranscriptional coupling of splicing factor recruitment and precursor messenger RNA splicing in mammalian cells. *Nat Struct Mol Biol* **13:** 815–822. doi:10.1038/nsmb1135

Ljungman M, Hanawalt PC. 1996. The anti-cancer drug camptothecin inhibits elongation but stimulates initiation of RNA polymerase II transcription. *Carcinogenesis* **17:** 31–35. doi:10.1093/carcin/17.1.31

Luco RF, Pan Q, Tominaga K, Blencowe BJ, Olivia M, Misteli T, Luco RF, Pan Q, Tominaga K, Blencowe BJ, et al. 2010. Regulation of alternative splicing by histone modifications. *Science* **327:** 996–1000. doi:10.1126/science.1184208

Mazin PV, Khaitovich P, Cardoso-Moreira M, Kaessmann H. 2021. Alternative splicing during mammalian organ development. *Nat Genet* **53:** 925–924. doi:10.1038/s41588-021-00851-w

McMahon DK, Anderson PAW, Bunting JB, Saba Z, Oakeley E, Carolina N, Anderson PAW, Bunting JB, Saba Z, Physiol AJ. 1994. C2C12 cells-biophysical, biochemical and immunocytochemical properties. *Am J Physiol* **5:** C1795–C1802. doi:10.1152/ajpcell.1994.266.6.C1795

Merkin J, Russell C, Chen P, Burge CB. 2012. Evolutionary dynamics of gene and isoform regulation in mammalian tissues. *Science* **338:** 1593–1599. doi:10.1126/science.1228186

Moulay G, Lainé J, Lemaitre M, Nakamori M, Nishino I, Caillol G, Mamchaoui K, Julien L, Dingli F, Loew D, et al. 2020. Alternative splicing of clathrin heavy chain contributes to the switch from coated pits to plaques. *J Cell Biol* **219:** e201912061. doi:10.1083/jcb.201912061

Nojima T, Gomes T, Grosso ARF, Kimura H, Dye MJ, Dhir S, Carmo-Fonseca M, Proudfoot NJ. 2015. Mammalian NET-seq reveals genome-wide nascent transcription coupled to RNA processing. *Cell* **161:** 526–540. doi:10.1016/j.cell.2015.03.027

Olson EN. 2006. Gene regulatory networks in the evolution and development of the heart. *Science* **313:** 1922–1927. doi:10.1126/science.1132292

Pan Q, Shai O, Lee LJ, Frey BJ, Blencowe BJ. 2008. Deep surveying of alternative splicing complexity in the human transcriptome by high-throughput sequencing. *Nat Genet* **40:** 1413–1415. doi:10.1038/ng.259

Park JY, Li W, Zheng D, Zhai P, Zhao Y, Matsuda T, Vatner SF, Sadoshima J, Tian B. 2011. Comparative analysis of mRNA isoform expression in cardiac hypertrophy and development reveals multiple post-transcriptional regulatory modules. *PLoS One* **6:** e22391. doi:10.1371/journal.pone.0022391

Protacio RU, Li G, Lowary PT, Widom J. 2000. Effects of histone tail domains on the rate of transcriptional elongation through a nucleosome. *Mol Cell Biol* **20:** 8866–8878. doi:10.1128/MCB.20.23.8866-8878.2000

Quinlan AR, Hall IM. 2010. BEDTools: a flexible suite of utilities for comparing genomic features. *Bioinformatics* **26:** 841–842. doi:10.1093/bioinformatics/btq033

Ray D, Kazan H, Cook KB, Weirauch MT, Najafabadi HS, Li X, Gueroussov S, Albu M, Zheng H, Yang A, et al. 2013. A compendium of RNA-binding motifs for decoding gene regulation. *Nature* **499:** 172–177. doi:10.1038/nature12311

Savkur RS, Philips AV, Cooper TA, Dalton JC, Moseley ML, Ranum LPW, Day JW. 2004. Insulin receptor splicing alteration in myotonic dystrophy type 2. *Am J Hum Genet* **74:** 1309–1313. doi:10.1086/421528

Schafer DA, Waddle JA, Cooper JA. 1993. Localization of CapZ during myofibrillogenesis in cultured chicken muscle. *Cell Motil Cytoskeleton* **25:** 317–335. doi:10.1002/cm.970250403

Schor IE, Gómez Acuña LI, Kornblihtt AR. 2013. Coupling between transcription and alternative splicing. *Cancer Treat Res* **158:** 1–24. doi:10.1007/978-3-642-31659-3_1

Sharma A, Nguyen H, Geng C, Hinman MN, Luo G, Lou H. 2014. Calcium-mediated histone modifications regulate alternative splicing in cardiomyocytes. *Proc Natl Acad Sci* **111:** E4920–E4928. doi:10.1073/pnas.1408964111

Singh RK, Xia Z, Bland CS, Kalsotra A, Scavuzzo MA, Curk T, Ule J, Li W, Cooper TA. 2014. Rbfox2-coordinated alternative splicing of Mef2d and Rock2 controls myoblast fusion during myogenesis. *Mol Cell* **55:** 592–603. doi:10.1016/j.molcel.2014.06.035

Spellman R, Smith CWJ. 2006. Novel modes of splicing repression by PTB. *Trends Biochem Sci* **31:** 73–76. doi:10.1016/j.tibs.2005.12.003

Sun S, Zhang ZUO, Fregoso O, Krainer AR. 2012. Mechanisms of activation and repression by the alternative splicing factors RBFOX1/2. *RNA* **18:** 274–283. doi:10.1261/rna.030486.111

Tang ZZ, Yarotskyy V, Wei L, Sobczak K, Nakamori M, Eichinger K, Moxley RT, Dirksen RT, Thornton CA. 2012. Muscle weakness in myotonic dystrophy associated with misregulated splicing and altered gating of Cav1.1 calcium channel. *Hum Mol Genet* **21:** 1312–1324. doi:10.1093/hmg/ddr568

Truebestein L, Leonard TA. 2016. Coiled-coils: the long and short of it. *Bioessays* **38:** 903–916. doi:10.1002/bies.201600062

Uhlén M, Fagerberg L, Hallström BM, Lindskog C, Oksvold P, Mardinoglu A, Sivertsson Å, Kampf C, Sjöstedt E, Asplund A, et al. 2015. Tissue-based map of the human proteome. *Science* **347:** 1260419. doi:10.1126/science.1260419

Ustianenko D, Weyn-Vanhentenryck SM, Zhang C. 2017. Microexons: discovery, regulation, and function. *Wiley Interdiscip Rev RNA* **8:** 10.1002/wrna.1418. doi:10.1002/wrna.1418

Van Nostrand EL, Freese P, Pratt GA, Wang X, Wei X, Xiao R, Blue SM, Chen JY, Cody NAL, Dominguez D, et al. 2020. A large-scale binding and functional map of human RNA-binding proteins. *Nature* **583:** 711–719. doi:10.1038/s41586-020-2077-3

Wang ET, Sandberg R, Luo S, Khrebtukova I, Zhang L, Mayr C, Kingsmore SF, Schroth GP, Burge CB. 2008. Alternative isoform regulation in human tissue transcriptomes. *Nature* **456:** 470–476. doi:10.1038/nature07509

Wang ET, Cody NAL, Jog S, Biancolella M, Wang TT, Treacy DJ, Luo S, Schroth GP, Housman DE, Reddy S, et al. 2012. Transcriptome-wide regulation of pre-mRNA splicing and mRNA

localization by muscleblind proteins. *Cell* **150:** 710–724. doi:10.1016/j.cell.2012.06.041

Wang ET, Ward AJ, Cherone JM, Giudice J, Wang TT, Treacy DJ, Lambert NJ, Freese P, Saxena T, Cooper TA, et al. 2015. Antagonistic regulation of mRNA expression and splicing by CELF and MBNL proteins. *Genome Res* **25:** 858–871. doi:10.1101/gr.184390.114

Wheeler TM, Lueck JD, Swanson MS, Dirksen RT, Thornton CA. 2007. Correction of ClC-1 splicing eliminates chloride channelopathy and myotonia in mouse models of myotonic dystrophy. *J Clin Invest* **117:** 3952–3957. doi:10.1172/JCI33355

Xu X, Yang D, Ding JH, Wang W, Chu PH, Dalton ND, Wang HY, Bermingham JR, Ye Z, Liu F, et al. 2005. ASF/SF2-regulated CaMKIIδ alternative splicing temporally reprograms excitation-contraction coupling in cardiac muscle. *Cell* **120:** 59–72. doi:10.1016/j.cell.2004.11.036

Xu SJ, Lombroso SI, Fischer DK, Carpenter MD, Marchione DM, Hamilton PJ, Lim CJ, Neve RL, Garcia BA, Wimmer ME, et al. 2021. Chromatin-mediated alternative splicing regulates cocaine-reward behavior. *Neuron* **109:** 2943–2966.e8. doi:10.1016/j.neuron.2021.08.008

Yeo G, Burge CB. 2004. Maximum entropy modeling of short sequence motifs with applications to RNA splicing signals. *J Comput Biol* **11:** 377–394. doi:10.1089/1066527041410418

Yu G, Wang LG, Han Y, He QY. 2012. ClusterProfiler: an R package for comparing biological themes among gene clusters. *Omi A J Integr Biol* **16:** 284–287. doi:10.1089/omi.2011.0118

Zhang J, Bahi N, Llovera M, Comella JX, Sanchis D. 2009. Polypyrimidine tract binding proteins (PTB) regulate the expression of apoptotic genes and susceptibility to caspase-dependent apoptosis in differentiating cardiomyocytes. *Cell Death Differ* **16:** 1460–1468. doi:10.1038/cdd.2009.87

MEET THE FIRST AUTHORS

Emma Hinkle

Hannah Wiedner

***Meet the First Author(s)* is a new editorial feature within *RNA*, in which the first author(s) of research-based papers in each issue have the opportunity to introduce themselves and their work to readers of *RNA* and the RNA research community. Emma Hinkle and Hannah Wiedner are co-first authors of this paper, "Alternative splicing regulation of membrane trafficking genes during myogenesis." Emma and Hannah are both fifth year PhD candidates in Genetics and Molecular Biology in Dr. Jimena Giudice's laboratory at the University of North Carolina at Chapel Hill. Emma's research focuses on investigating the interplay between mechanotransduction and alternative splicing in skeletal muscle, and Hannah's research focuses on the regulatory mechanisms of alternative splicing during muscle development and their functional outputs.**

What are the major results described in your paper and how do they impact this branch of the field?

Skeletal and cardiac muscle exhibit high levels of alternative splicing in membrane trafficking genes; various groups have demonstrated that this contributes to tissue maturity. Here we discover that the RNA-binding proteins (RBPs), polypyrimidine tract binding protein 1 (PTBP1) and quaking (QKI), regulate the splicing of membrane trafficking genes. Further, we describe a previously unknown phenomenon whereby chromatin-modifying drugs impact both alternative splicing and RBP expression. These findings impact the field of both RNA and skeletal muscle by expanding our understanding of alternative splicing regulation in striated muscle tissues.

What led you to study RNA or this aspect of RNA science?

EH: Before beginning graduate school, I was interested in DNA, but I soon realized that RNA is the molecule that gets things done in the cell! With my interest in mechanotransduction (how cells sense mechanical signals and create biochemical cues), I find it fascinating that skeletal muscle undergoes alternative splicing changes as well as mechanical changes during development to mature the tissue.

HW: One of the questions that initially fascinated me in biology was "if humans develop from a single cell, how are cells from different bodily tissues so unique?" For example, cells in our bones look and function differently than brain cells, yet they contain essentially the same genetic material. My pursuit to answer this question led me to become fascinated by the intricacies of gene expression networks, feedback loops, and the regulatory mechanisms involved in tissue development.

During the course of these experiments, were there any surprising results or particular difficulties that altered your thinking and subsequent focus?

We began working on experiments for this paper during our lab rotations during the first year of our PhD program nearly four years ago! Because the COVID-19 pandemic began in the middle of this project, we faced difficulties (as many scientists did) in completing the necessary experiments, which set us back some. However, it also provided the opportunity for us to grow as scientists and form stronger collaborative skills to complete this work.

If you were able to give one piece of advice to your younger self, what would that be?

EH: Our lab motto is "little by little," meaning that by making small steps of progress every day we will meet our goals in the long run.

Continued

I would tell my younger self that it's better to be faithful every day in work instead of mistakenly thinking that you must accomplish something big every day. Those exciting accomplishments only happen once in a while, but they are due to the faithfulness and perseverance exhibited in the mundane.

HW: If I could give any piece of advice to my younger self, I would say "have more confidence in your scientific ideas!" I think it's easy when you're young to view scientists as mega-geniuses who know everything about how the world works. In reality, we know far less about the world compared to the vast chasm of unknowns (which is what makes science fun and worthwhile for me). There will always be so much room for good, creative, and testable ideas in science!

What are your subsequent near- or long-term career plans?

EH: In college I majored in Genetics and English and through graduate school I have enjoyed communicating my science to others. It is very satisfying to take a complex scientific concept and break it down into an analogy that anyone can understand. I'm planning to pursue a career in Medical Communications post PhD!

What were the strongest aspects of your collaboration as co-first authors?

EH: Hannah and I really prioritized communication and being on the same page. This made it easy to discuss various aspects about the paper and come up with a plan that we both agreed with. Both of us are kind and understanding people so that helped our collaboration to be a positive experience.

HW: My favorite aspect of working together was having the opportunity to exchange skills, perspectives, ideas, and tools that I would not have otherwise known about. Especially because Emma and I are early-stage researchers, understanding how to integrate perspectives, work cohesively, and adapt will serve us well for the rest of our careers. It's a rare experience to have and it's one I will cherish as Emma and I prepare to graduate soon!